



OPEN ACCESS

EDITED BY

Thiago da Silva Marinho,
Universidade Federal do Triângulo
Mineiro, Brazil

REVIEWED BY

Hermínio Ismael de Araújo-Júnior,
Rio de Janeiro State University, Brazil
Fernando Erthal,
Federal University of Rio Grande do Sul, Brazil

*CORRESPONDENCE

Michelangelo Bisconti,
✉ michelangelo.bisconti@unich.it

RECEIVED 10 January 2025

ACCEPTED 26 March 2025

PUBLISHED 22 April 2025

CITATION

Bisconti M, Monegatti P, Raineri G, Tartarelli G
and Carnevale G (2025) Taphonomy and
whale-fall analysis of the Tortonian baleen
whales from the Stirone river, Emilia Romagna
(northern Italy).

Front. Earth Sci. 13:1558428.

doi: 10.3389/feart.2025.1558428

COPYRIGHT

© 2025 Bisconti, Monegatti, Raineri, Tartarelli
and Carnevale. This is an open-access article
distributed under the terms of the [Creative
Commons Attribution License \(CC BY\)](#). The
use, distribution or reproduction in other
forums is permitted, provided the original
author(s) and the copyright owner(s) are
credited and that the original publication in
this journal is cited, in accordance with
accepted academic practice. No use,
distribution or reproduction is permitted
which does not comply with these terms.

Taphonomy and whale-fall analysis of the Tortonian baleen whales from the Stirone river, Emilia Romagna (northern Italy)

Michelangelo Bisconti^{1,2*}, Paola Monegatti³, Gianluca Raineri⁴,
Giandonato Tartarelli⁵ and Giorgio Carnevale⁶

¹Dipartimento di Ingegneria e Geologia, Università degli Studi "G. D'Annunzio" di Chieti-Pescara, Chieti, Italy, ²San Diego Natural History Museum, San Diego, CA, United States, ³Dipartimento di Scienze Chimiche, della Vita e della Sostenibilità Ambientale, Università degli Studi di Parma, Parma, Italy, ⁴Museo 'Mare antico e biodiversità', Salsomaggiore Terme, Italy, ⁵Scuola Normale Superiore, Pisa, Italy, ⁶Dipartimento di Scienze della Terra, Università degli Studi di Torino, Torino, Italy

Introduction: The taphonomy of three balaenopterid skeletons is examined in order to describe the traces left by whale fall communities. The whale specimens include two partial skeletons and an isolated periotic; one of the partial skeletons is the holotype of *Plesiobalaenoptera quarantellii*, while the other two specimens represent two indeterminate balaenopterid species. The high number of trace fossils observed in these specimens was not observed in previous paleontological records of whale fall communities. The diversity of the trace fossils and the broad stratigraphic context in which the assemblages are included are investigated in order to investigate into the origin and evolution of the specialized whale fall communities since the Neogene.

Methods: Macrophotographs, three-dimensional modeling from photogrammetry and laser scanner examinations of the specimens were used to analyze the diversity of trace fossils observed on the bones of the balaenopterids. Biostratigraphic analyses of the outcrops where the specimens were discovered were realized to constrain the ages of the specimens and to reconstruct paleoecological characters of the sites. Additionally, analyses of fish otoliths, mollusc shells and microfossils were carried out to refine the ecological setting of the sites.

Results: The partially articulated skeletons were affected by intense bioerosion and disarticulation that displaced several bones before the final burials. Trace fossils found on the whale bones include shark bite traces, *Trypanites*, *Gastrochaenolites*, *?Meandropolydora* and *Gnatulichnus* ichnogenera documenting an intense exploitation of the energy reservoir represented by these carcasses. The biostratigraphic analysis of the site supports a Late Miocene (Upper Tortonian) age and shows presence of post-depositional processes. These included micro-faulting that acted on the whale bones and, in one case, provided forces able to deform a lumbar vertebra. Fish otoliths, mollusc shells and microfossils are consistent in supporting a c. 100 m deep inner shelf deposit.

Discussion: Absence of chemoautotrophic molluscs from the present whale falls confirms that water depth may be the main determinant of the presence of these highly specialized species, that flourish in anoxic environments, because decomposition at shallow depths may still occur in presence of high Oxygen

concentrations. Those described herein are the most dense ensembles of traces documenting whale falls communities in the Late Miocene described up to now.

KEYWORDS

Balaenopteridae, biostratigraphy, Emilia Romagna, Miocene, *Plesiobalaenoptera*, Salsomaggiore Terme, taphonomy, Tortonian

1 Introduction

The carcasses of large marine mammals like baleen whales undergo complex dismantling processes carried out by communities formed by vertebrate and invertebrate species (hereinafter, SCCDs) that are specialized in carcass decay (e.g., Li et al., 2022; Smith et al., 2015). Researches published in the last 2 decades have illuminated the subsequent steps followed by SCCDs in the exploitation of the enormous energy reservoirs represented by the bodies of large cetaceans (e.g., Danise et al., 2014; Smith et al., 2015; Glover et al., 2010; Dahlgren et al., 2006; Smith and Baco, 2003; Allison et al., 1991). Specialized invertebrate species, like the polychaete annelid *Osedax*, have been described for the first time from surveys of decaying whale carcasses leading to the idea that dead baleen whale bodies constitute energy islands that occasionally provide abundant food to a number of marine species (Alfaro-Lucas et al., 2017; Braby et al., 2007; Dahlgren et al., 2004).

The origin and evolution of the SCCDs is still poorly known but the fossil record may help in deciphering when and where these communities originated. Works on Mesozoic marine reptiles demonstrated that *Osedax*-like species were present among the communities developed around the dead bodies of plesiosaurs and ichthyosaurs (e.g., Jamison-Todd et al., 2023; Danise et al., 2014). More or less complex community structures have been described from Neogene sites bearing mysticetes in South America and Europe showing different SCCD compositions and different paths of decay of whale carcasses in a variety of paleoenvironmental contexts. Dominici et al. (2009), in particular, provided an extensive analysis of the mollusc communities found around whale skeletons from the Pliocene of several Italian sites. They concluded that SCCDs were certainly present in Mediterranean in the early and late Pliocene. Dominici et al. (2020) updated the previous dataset by including additional sites and provided a theoretical context where SCCD development through time was incorporated. In particular, they linked preservational styles of mysticete skeletons to sedimentary characteristics and suggested that the preservation potential increases by shortening the time intercurring between the deposition of the body on the marine floor and its complete burial. This suggests that carcasses deposited on deep floor remain on the surface for longer time than those deposited in near-shore areas, suggesting that the preservation potential of whale skeletons deposited in abyssal contexts is very reduced. Moreover, they concluded that preservation potential of whale carcasses deposited in shallow floors depends on their quick burial thereby evidencing the potential existence of a causal link between preservation quality and sedimentation rates.

This last conclusion was put into discussion by Bosio et al. (2021) who found no correlation between sedimentation rates calculated in sites of the Pisco Formation in Peru and preservation of whale skeletons in the field. Bisconti et al. (2021a) described the

taphonomy of Pliocene mysticetes from Piedmont; that research resulted in the observation that different preservational styles are represented in a relatively limited area and in the same sedimentary basin. The presence of SCCDs was occasionally reported in the Piedmontese specimens, including the holotype of *Marzanoptera tersillae* (Bisconti et al., 2021b), and in the holotype of *Charadrobalaena valentinae* (Bisconti et al., 2023a) from Emilia Romagna. Unpublished work on a disarticulated balaenopterid from the early Pliocene of southern Tuscany is currently in progress with the description of a complex SCCD (Bisconti et al., 2023b; Scotton et al., 2020; 2018) while borings attributed to *Osedax* were documented in Pliocene whale bones by Higgs et al. (2012).

Taphonomic analyses of Miocene and Oligocene whale falls have been carried out in the past 2 decades providing important context in this field (see, for example, Bisconti et al., 2021a; Higgs et al., 2012; Kiel et al., 2010a; Dominici et al., 2009) but additional case studies would be of great help to better understand origin, diversity and evolution of these specialized communities. In this paper, we describe the taphonomy of three balaenopterid specimens from Late Miocene sediments outcropping at the La Bocca area in the Scipione Ponte locality along the east and west banks of the Stirone River, Emilia Romagna, northern Italy (Figure 1).

In 1988, the Emilia-Romagna Region instituted the Stirone Regional River Park with the distinctive aim of protecting and enhancing the geo-paleontological heritage exposed in the bed of the Stirone River. An important step, which led to the establishment of a true paleontological museum (today Museo Mare Antico e Biodiversità; hereinafter MuMAB), was the discovery of fossil skeletons of the three balaenopterids discussed in the present paper from the Miocene deposits of the Stirone River. The discoveries started from the late 1980s and were paralleled by finds of additional skeletons from the Pliocene of other localities (Freschi and Raineri, 2014).

The balaenopterids documented herein were discovered by the late Raffaele Quarantelli in the 1980s and became one of the main elements of attraction of the MuMAB of Salsomaggiore Terme (Figure 2). The specimens are late Miocene in age (Bisconti, 2010; Bisconti et al., 2022) and include: (a) the holotype of *Plesiobalaenoptera quarantellii*, (b) a disarticulated balaenopterid specimen still under study (Bisconti, 2003), and (c) the periotic of a large-sized balaenopterid (Bisconti et al., 2022). We examined these three specimens looking for information about the history of the corresponding carcasses from death to burial with the aim to analyze taphonomic processes active in the late Miocene of central Mediterranean, a few million years before the Messinian salinity crisis at the end of the Miocene. Moreover, we examined the exploitation of food/energy resources by necrophagous organisms based on the energy availability provided by the whale carcasses. These three specimens represent the whole record of Late Miocene mysticetes from northern Italy while nearly contemporaneous

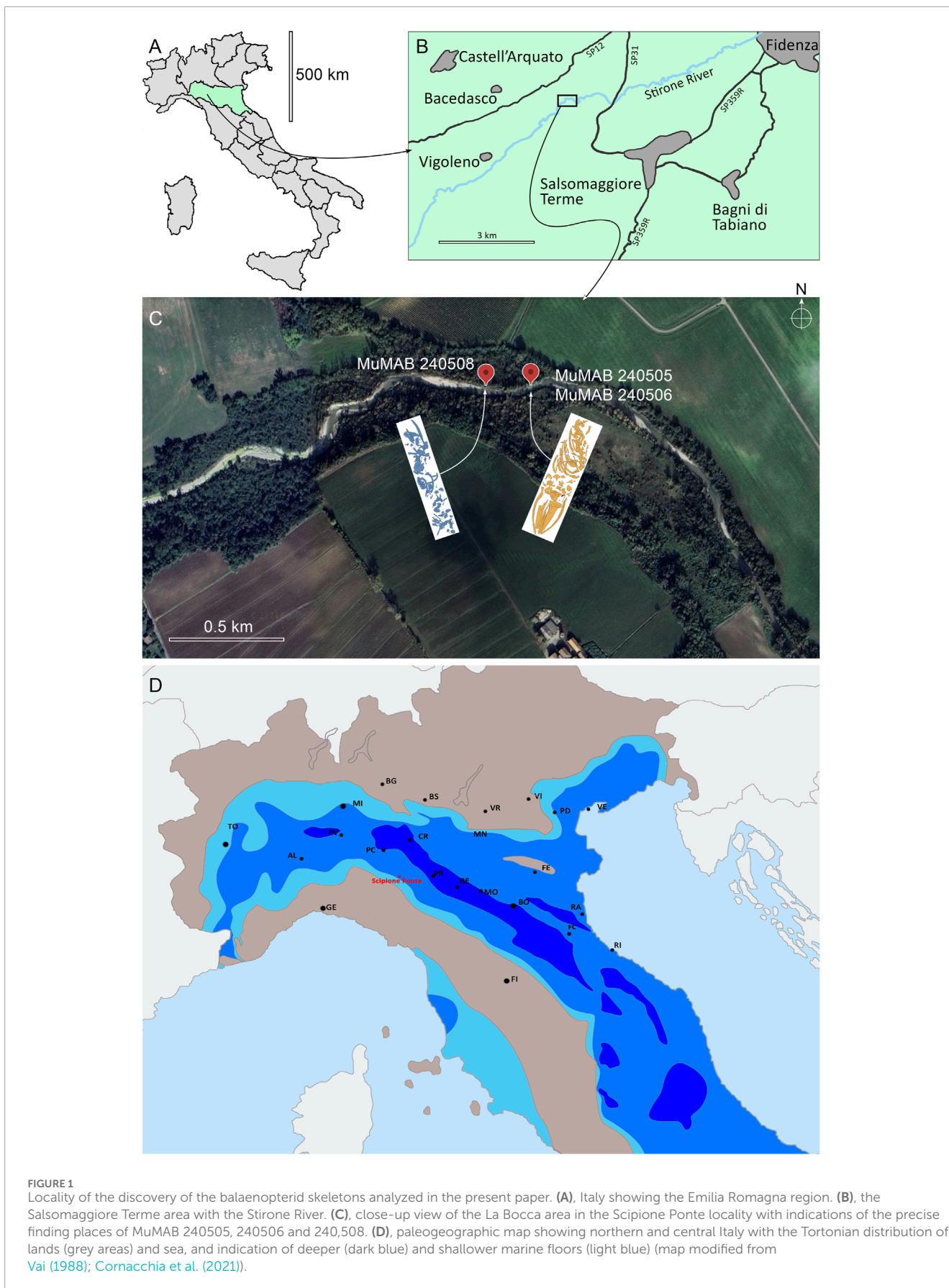




FIGURE 2

Historical pictures showing phases of the excavation and extraction of MuMAB 240505, *Plesiobalaenoptera quarantellii* holotype. (A), excavation of the right mandibular ramus; note that it was rotated about 90° inward and that it is not in apparent connection with the remainder of the skull. (B), extraction of the rostrum and both mandibular rami; note that the complex formed by rostrum and mandibular rami is covered and protected with a plaster jacket, that both mandibular rami are strictly adherent to the rostrum, that the rostrum is upside down as demonstrated by the central protrusion (black arrowhead) indicating the vomerine crest, and that rostrum and mandibular rami were positioned in a separate block with respect to the neurocranium. (C), early exhibition of the skeleton showing the rostrum upside up and the right mandibular ramus showing the original laying pattern as in (A). Courtesy of the Municipality of Salsomaggiore Historical Archive.

mysticetes are known from the Pietra Leccese Formation of southern Italy (see Bisconti, 2003; Bisconti and Varola, 2006; 2000). Early and middle Miocene specimens are represented by *Atlantictetus lavei* (Burdigalian, 19–16 Ma, Piedmont; Bisconti et al., 2021c) and *Titanocetus sammarinensis* (Serravallian, c. 13 Ma, San Marino; Bisconti, 2006) and come from different sedimentary realms that are not analyzed here.

The goals of the present paper are, therefore, the description of the trace assemblage found in association with the three balaenopterid skeletons from the Stirone river (systematic paleoichnology *sensu* Jacobsen & Bromley, 2009), the analysis of this assemblage in the broader context of the paleoecological reconstruction of the site, the comparisons between our results and what is currently known about the evolution of the whale-fall communities throughout the Cenozoic. Given the good preservation of the fossils investigated here, we think that our results will significantly increase our knowledge about the evolution of the whale-fall communities and marine paleoecology.

2 Stratigraphic and paleoenvironmental setting

The Miocene outcrops along the Stirone river (Figure 1), upstream of Scipione Ponte, belong to the Epiligurian succession, constituted by “tectonically controlled turbidite and slope deposits” that settled between the middle Eocene and the early Messinian in a piggy-back, wedge-top basin (Artoni et al., 2004). The Messinian hypohaline deposits occur at the top of this succession. In particular,

the sediments outcropping along the banks of the Stirone River near the La Bocca locality, in which the cetaceans were found, belong to the “Scipione Member” (Termina Formation, upper Serravallian-lower Messinian). These sediments are strongly faulted, fossiliferous, and bioturbated locally. The biostratigraphic data indicate a Tortonian age for the succession (Zermani, 2001; Lin et al., 2017). Recent biostratigraphic analysis based on planktonic foraminifera allowed to refer these sediments to the upper Tortonian/lower Messinian (N17, *Globorotalia suterae*/*Globorotalia mediterranea* Zone), most likely to the upper Tortonian NN10 calcareous nannofossil zone (ranging from c. 9.5 to c. 8.5 Ma; Lin et al., 2017). The Upper Tortonian age for this succession is also confirmed by the diversity of malacofauna present, typical of the upper Tortonian in terms of both biogeographic and stratigraphic distributions (Monegatti and Raffi, 2010).

The succession is characterized by an alternation of glauconitic-silty sands and fossiliferous sandy silts, lacking evident stratification probably due to bioturbation. A biocalcarenic layer, rich in brachiopods, bivalves, gastropods, and corals, is present in the lower part. All the fossil cetaceans were found in the sediments below the biocalcarenic layer. In particular, the holotype of *Plesiobalaenoptera quarantellii* and the isolated periotic are in the glauconitic sands, and the indeterminate specimen in the sandy silts. The sandy fraction increases above the calcarenite, as does the fossil content. In fact, the macrofauna becomes more abundant above the calcarenite layer, particularly in areas with major concentrations of glauconite (Zermani, 2001).

In the literature, the Member of Scipione has been considered related to the transition between the inner and outer shelf

(Artoni et al., 2004). The lack of data about the facies and the quantitative data on benthic associations prevents a detailed paleoenvironmental reconstruction. Moreover, the qualitative studies on molluscs, which represent the dominant component of the benthic fauna (Marasti, 1973) in the biocalcarene and overlying sediments, suggest a reference to a distal circalittoral environment. This is based on the most common species, such as *Ancillaria glandiformis* (Lamarck), *Thracia convexa* (Wood), *Clavilithes klipsteini* (Michelotti), *Clavatula semimarginata* (Lamarck), and *Amusium cristatum* (Bronn), along with the presence of solitary corals and brachiopods. This interpretation agrees with the Plancton/Benthos Foraminifera ratio, which indicates an average depth of 100 m throughout the succession (Zermeni, 2001).

A rather diverse assemblage of moderately preserved saccular otoliths has been collected in the sediments surrounding the whale skeleton, corroborating the paleoenvironmental inference hypothesis based on the molluscs. Rare teeth pertaining to an indeterminate species of the requiem shark genus *Carcharhinus* have been also collected. The otolith assemblage is dominated by far by lanternfishes of the genera *Diaphus* (*Diaphus* spp.), *Hygophum* (*Hygophum* sp.), *Lobianchia* (*Lobianchia* cf. *dofleini*) and *Benthoosema* (*Benthoosema* aff. *glaciale*), as well as by two silvery pout species (*Gadiculus argenteus*, *G. labiatus*) and the acropomatiform *Verilus mutinensis*. Several other taxa have been also recognized, including the conger eels *Ganthopsis* sp. and *Rhynchoconger* cf. *pantanelii*, lanternfishes *Notoscopelus elongatus* and *Scopelopsis pliocenicus*, carapid *Echiodon* sp., red brotula *Brosomphycis* sp., the forbear *Phycis* sp., slimehead *Hoplostethus praemediterraneus*, deepwater cardinalfish *Epigonus* sp., sparid *Pagellus* sp., red bandfish *Cepola* cf. *macrophthalma*, scabbardfish *Lepidopus* sp., plus a few poorly preserved otoliths of gobies and of a single flatfish.

In addition, the abundance of glauconite in silty sands is one of the most sensitive markers of low sedimentation rates in marine environments and, as a consequence, it is generally associated with sedimentation breaks of varying importance, predominantly in marine shelf and slope deposits (Amorosi, 1997). The concentration of glauconite in specific levels and the highly variable degree of preservation of macrobenthos and microfossils suggest that this succession was deposited in an unstable distal shelf environment, typical of environments in active tectonic areas. The instability was attributable to changes in sedimentation rates associated with reworking and storms related to tectonically controlled sea level changes.

3 Materials and methods

3.1 Materials examined

MuMAB 240505, *Plesiobalaenoptera quarantellii*, holotype. The specimen includes the rostrum, part of the neurocranium, two periotics and two tympanic bullae, part of the hyoid, two cervical and ten lumbar vertebrae, and 15 ribs. Anatomical description and phylogenetic analysis were provided by Bisconti (2010); historical account of the discovery was provided by Freschi and Raineri (2014). It was discovered by the late Raffaele Quarantelli and Avio Martini in 1985 on the west bank near the La Bocca area in Scipione Ponte (Salsomaggiore Terme), in Upper Miocene

deposit. From a phylogenetic point of view, this species is part of a clade including *Parabalaenoptera*, *Fragilicetus*, '*Megaptera*' *hubachi* and a possible *Plesiobalaenoptera* sp. from South Africa (Bisconti et al., 2024; Gowender et al., 2016).

MuMAB 240506, Balaenopteridae indet (under study). The specimen includes part of the skull, both the periotics and tympanic bullae, left scapula, three cervical, two lumbar and three indeterminate vertebrae, six ribs and ten vertebral epiphyses. A general overview of the specimen was provided by Bisconti (2003). It was discovered in the same Miocene sediments like MuMAB 240505 near La Bocca, along the west bank of the Stirone River.

MuMAB 240508, Balaenopteridae indet. The specimen includes the left periotic lacking the posterior process. The anatomical description was provided by Bisconti et al. (2022). The specimen was discovered during the preparation of the holotype of *Plesiobalaenoptera quarantellii* and was preliminarily indicated as an 'alien' periotic by Bisconti (2010); therefore it is from the east bank of the Stirone River. This specimen was then described and considered as derived from a large-sized balaenopterid whale (Bisconti et al., 2022).

The specimens were found along the Stirone River in Emilia Romagna, northern Italy. This region was part, together with other Italian regions, of a marine realm that, in the Early Miocene represented an uninterrupted seaway south to the Alps (Vai, 1988). During the Tortonian, this seaway was closed making it a deep and wide gulf known as the Padan Gulf (Figure 1D) (Cornacchia et al., 2021; Vai, 1988). The balaenopterids studied here come from the central part of the Tortonian Padan Gulf.

3.2 Photogrammetry and three-dimensional model

The balaenopterid whales were photographed in three sessions by using a full frame Nikon Z7 mirrorless photocopier with a Nikkor Z 24–70 mm f/4 and a Tamron 90 mm f/2.8 Di macro VXD lenses. Lighting was provided by a Nikon SB600 speedlight flash mounted on the photocopier. Images were adjusted for contrast, saturation and light in Adobe Photoshop 26.1.0 (2024) and DxO Nik Collection Viveza 7. The photogrammetry of MuMAB 240505 was assembled from 201 images and that of MuMAB 240508 was assembled from 169 images in Agisoft Photoscan software (www.agisoft.com).

MuMAB 240505 was scanned with the Artec Spider surface scanner (Artec group; Luxembourg). Artec Spider is a hand-held, high-resolution structured light technology 3D surface scanner with a 3D resolution of 0.1 mm and a 3D point accuracy of 0.05 mm. The speed of capture is 8.0 fps at maximum and the scanner was able to collect in real-time frames containing geometrical information and frames containing colorful high resolution texture information for texture mapping. We followed a standardized scanning protocol acquiring raw data with multiple passes of the scanner. These raw data were then elaborated with the dedicated software Artec Studio Professional (v. 15.0) to clean, align and refine the point cloud. This discrete point cloud in space is the base of the software to construct a surface model of the object by forming a triangular patch. This model was finally exported as a .ply file.

3.3 Biostratinomy

The biostratinomic study was assessed following the methods outlined by Bisconti et al. (2021a), Bisconti et al. (2021b) that include: 1) assessment of skeletal completeness: comparison between the bone counts of the studied specimens and the generalized balaenopterid skeletons reconstructed by Bisconti et al. (2021a); 2) assessment of duration of eventual floating of carcass after death based on presence/absence of mandibular rami and forelimbs in the studied specimens (see Boessenecker, 2013); 3) assessment of articulation pattern: comparisons between the articulations found in the studied specimens and the number of articulations predicted from the generalized balaenopterid skeleton; 4) assessment of bone transport: count of transverse and neural processes of the vertebrae, search for abraded surfaces; 5) assessment of vertebrate exploitation of the carcasses: search and count of eventual shark bite traces on the bones, and search and count of fish feeding traces (the classification of shark bite traces follows Collareta et al., 2017 which extensively reported the results from Cigala-Fulgosi, 1990); 6) assessment of invertebrate exploitation of the carcasses: search and count of eventual crab signs and perforations that may be attributed to *Osedax*-like annelids, search of eventual barnacle remains and barnacle scars on the bones of the investigated specimens, search and taxonomic and paleoecological analyses of molluscs found in close proximity to or on the whale bones; 7) comparison of the results of the biostratinomic analysis with the general paleoecological conditions at the sites of carcass depositions as reported in chapter two.

See Bisconti et al. (2021a), Bisconti et al. (2021b) for further explanations of the methods.

4 Results

4.1 Taphonomy of MuMAB 240505, holotype of *Plesiobalaenoptera quarantellii*

4.1.1 Preservation and distribution of the bones

A total of 49 bones are observed in the skeleton representing the 26.2% of the total predicted bones for a generalized balaenopterid (Supplementary Figure S1). Therefore, only about one-fourth of the skeleton is preserved in the holotype of *Plesiobalaenoptera quarantellii*.

According to Boessenecker (2013), the presence, in this skeleton, of both mandibular rami and part of a forelimb (as represented by the distal portion of one ulna and by a part of a scapula) supports the hypothesis that the carcass did not float for long time after the death.

The analysis of the dispersion of the bones of the holotype of *Plesiobalaenoptera quarantellii* shows that the skeleton was disturbed after the deposition on the sea floor (Figure 3). Most of the articulations are lost and only the sequence of the lumbar vertebrae is maintained. Indeed, only seven articulations are preserved from a predicted total of 152 (4.6%); however, the bones are located approximately in a way reminiscent of the original anatomical disposition. However, the main axes of these vertebrae are rotated anteriorly of about 90° so that the anterior faces of their epiphyses are immersed within the matrix and the posterior faces are exposed. Most of the ribs are located in an area close to the lumbar vertebrae

and their distribution is substantially regular with the rib shafts parallel to each other in most cases. Only a few ribs are inconsistently distributed with respect to this pattern. The superimposition of some ribs on other ones shows that the pressure exerted by the overcharging sediment was not relevant since there are not abundant fractures along the transverse axes of the long bones and the bones maintain most of their integrity.

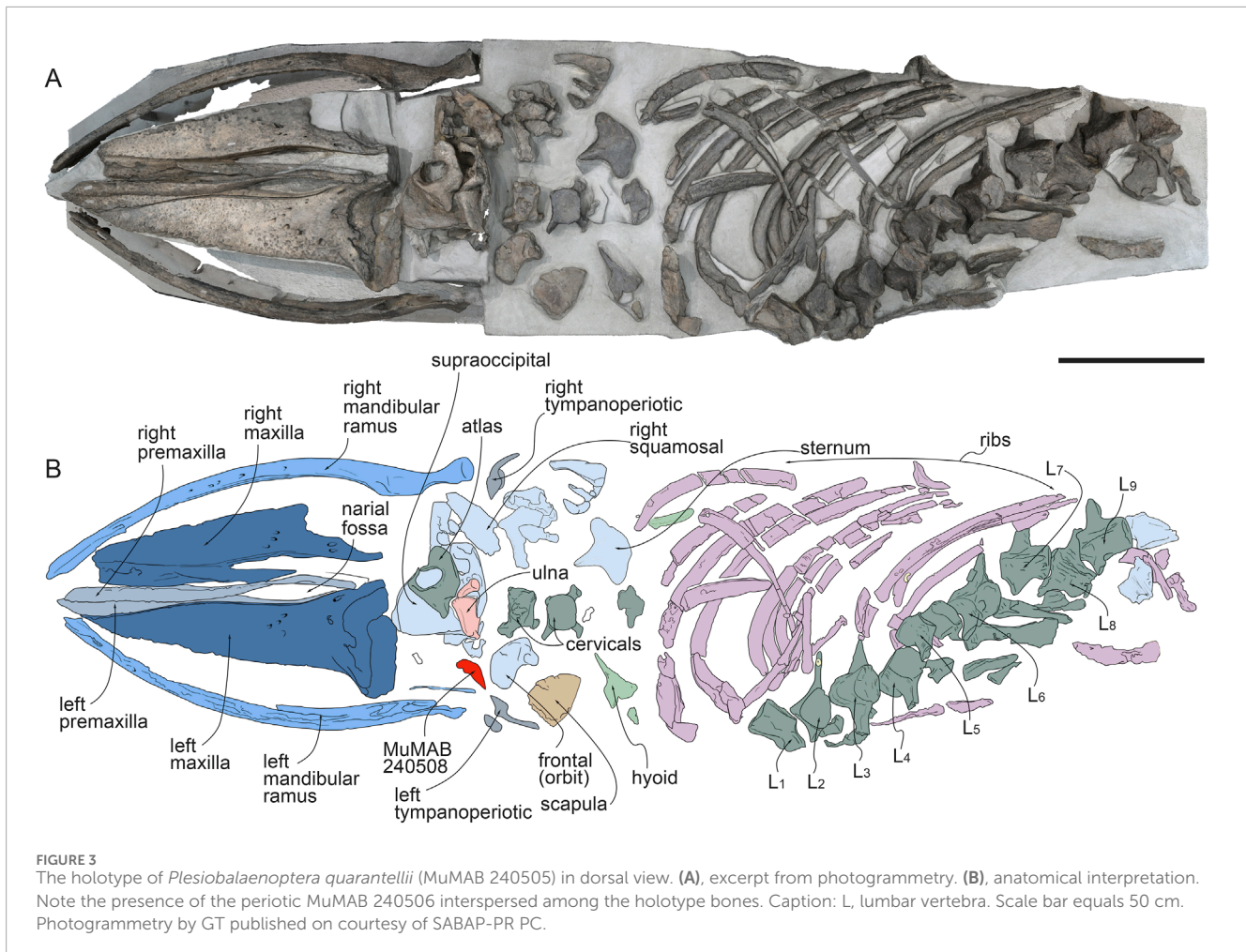
Despite the general lack of signs of strong pressure, the neural processes of the lumbar vertebrae are broken off and separated from the vertebral bodies; this suggests that some sort of weight was acting on the skeleton. Judging from the exposure of the ventral surfaces of the rostrum and the vertebrae, it is suggested that the whale body was upside down on the sea floor at the time of the burial although the presence of encrusting molluscs on the dorsal surface of the rostrum is a proof that the skeleton was exposed upside up for long time. It is therefore possible that there was a violent rotation of the body at a moment when part of the tendinous and muscular components were still in place; that movement could have been responsible of the breakage of the neural processes of the vertebrae but did not influence the preservation of the transverse processes.

The vertebral epiphyses are still in place and none of them is detached from the vertebral bodies; only the epiphyses of the ninth lumbar vertebra shows a partial detachment. All the transverse and neural processes are in place suggesting that the vertebrae were scarcely moved from their life position and did not undergo transport, as confirmed by their distribution that is consistent with the original anatomical sequence.

Unfortunately, there is not any field note about the original dispersion of the bones. However, the preparation preserved the postcranial skeleton still partially embedded in the original sedimentary matrix and for this reason we are sure that the whole postcranial is currently representing the field distribution of the bones. The same is not true about the rostrum and the mandibular rami. According to one of the discoverer (Avio Martini, personal communication) and based on a couple of pictures taken during excavation and extraction of the specimen, at least the right mandibular ramus was rotated of about 90° inward and the rostrum was upside down (Figures 2A, B). Judging from Figure 2B, both mandibular rami were located under the palate, but it is not clear how this arrangement can agree with the single right mandibular ramus shown in Figure 2A. We cannot exclude that both mandibular rami were packed together with the rostrum for easier transport outside the excavation site. The rostrum was then polished and rotated, and the mandibular rami were positioned parallel to the maxillae for exhibition (Figure 2C). We have no chance to know the exact position of these bones with respect to the rest of the postcranial skeleton and for this reason we represent the skeleton as it is currently on display. However, in the biostratinomic analysis, we need to take in mind that the rostrum was rotated at a certain point after it was disarticulated from the neurocranium and after being settled and exploited by invertebrate saprophagous animals. Therefore, we conclude that the rostrum relied on the sea floor for a certain period upside up, it was subject to exploitation and then rotated to become exposed upside down.

4.1.2 Whale-fall analysis: opportunistic stage

The overall longitudinal disposition of the bones follows the general vertebrate scheme. The thoracic region, however, is



particularly damaged. The lack of the thoracic vertebrae and of the forelimbs (only one fragment of the posterodorsal corner of the scapula and one fragment of the radius are present) suggests that these portions were particularly disturbed. We found a long shark bite trace in the middle section of the left mandibular ramus (Figures 4, 5) which is consistent with a large shark tooth lacking serration. Two additional shark bite traces are found at about 15 cm from the posterior end of the left mandibular ramus (Figures 4, 5). The anterior of these marks shows a posterior concavity and the posterior one shows an anterior concavity. With respect to the classification of shark bite traces provided by Collareta et al. (2017), the first trace is a type V and the second and third ones are attributed to type I.

A series of shark bite traces are observed in the lateral and dorsal surfaces of the right mandibular ramus (Figures 6, 7); all these marks are oriented transversely with respect to the longitudinal axis of the bone. The posterior trace is attributed to the type V and shows a similar pattern that can be attributed to an *Isurus* tooth characterized by lack of serration. The other shark bite traces are less sharp and cannot be easily classified.

No additional shark bite traces are observed in this specimen.

Traces of invertebrate feeding are well distributed in the whole skeleton. In the rostrum, mm-sized to cm-sized borings

are observed in the whole maxillae and premaxillae (Figure 8, Supplementary Information Model S1). The external borders of the maxillae are almost entirely destroyed due to the presence of large-sized borings. Many borings coalesce and form larger borings. The outline of the mm-sized borings is approximately elliptical resembling those of the extant *Osedax* polychaete annelid frequently observed in whale-fall communities developed on whale carcasses deposited on deep sea floors. The smaller borings are assigned to the ichnogenus *Trypanites*. The larger borings resemble those attributed to the ichnogenus *Gastrochaenolites*. Borings are also abundant in the mandibular rami and in the atlas (Figure 9). Also the ribs appear widely bioeroded and perforated; large quantities of small-sized holes are inferred in the ribs based on the distribution of sediment fillings of the borings themselves (Figure 10). In the vertebral bodies the borings are less numerous.

Additional traces of invertebrate feeding activities include the following: 1) a series of intricate, tiny, overlapping and intercrossing sulci located on the left mandibular ramus slightly anterior to the position of the condyle that could be assigned to the ichnogenus *Meandropolydora* (Figure 7D), 2) a single trace located in the right mandibular ramus slightly below the base of the coronoid process that includes a series of parallel sulci (Figures 7B, C), and 3) a linear excavation on an indeterminate skull bone (Figures 9E, F).



FIGURE 4

Opportunistic stage of the whale fall associated to MuMAB 240505. (A), left mandibular ramus showing the portions that are highlighted in the subsequent boxes. (B), type VI shark bite trace. (C), type I shark bite traces (arrowheads). (D), *Gnathichnus* sp. feeding traces. (E), *Gastrochaenolithes* sp. (white arrowheads) and borings attributed to *Osedax*-like bone-eating worms (red arrowhead). Pictures by MB published on permission of SABAP-PR PC.

All these cases are referred to as invertebrate feeding activities. The presence of the ichnogenera *Gastrochaenolithes*, *Trypanites* and *Meandropolydora* indicates a long *post-mortem* period of exposition before the early diagenetic stage. Interestingly, no traces are observed in the periotics and tympanic bullae of this specimen probably because these bones are among the hardest to penetrate even though cases of borings of tympanic bullae are known in the literature (Higgs et al., 2014).

4.1.3 Whale-fall analysis: Reef stage

Mollusc shells are found attached to the balaenopterid bones in several anatomical sectors of the skeleton. A valve of the bivalve *Lopha* cf. *plicatula* is observed approximately at the middle of the left maxilla (Figure 10A); this specimen, with a maximum diameter of c. 70 mm, encrusts the whale rostrum suggesting that this portion was exposed on the sea floor for a long time span (Carlucci et al., 2010; Walne, 1958) before being rotated. Additional ostreid shells are observed in other portions of the maxilla (Figure 10B), and on the left lateral process of the maxilla (Figure 10C). Small-sized shells are strictly associated with the ribs (Figures 10D,E). A large pectinid shell akin to *Chlamys* cfr. *spinulosa* in possible life position is found steadily attached to

the medial surface of the left mandibular ramus (Figure 10F). The presence of abundant epifaunal mollusc shells suggests that the bones were extensively colonized by these organisms, and that most of the skeleton likely provided a hard substrate for encrusting molluscs. No traces of barnacles or barnacle scars were observed.

4.1.4 Post-depositional processes

Post-depositional changes occurred because of the presence of several faults and micro-faults. Two main faults cross the rib *ensemble* and one lumbar vertebra. Because of that, the ribs are subdivided into several segments that were moved together with the matrix encasing them due to fault-related tectonic activity. It is possible to observe how the faults acted on the rib distribution in Figures 11A, B. The faulting of the matrix is pervasive, and this is testified by the presence of parallel micro-faults regularly distributed along the longitudinal axes of ribs, mandibular rami and vertebrae (Figure 11C) whose orientation is parallel to the two main faults described above. One fault crossed the ninth lumbar vertebra resulting in a plastic deformation; the centrum was rounded and the longitudinal axis of the vertebra changed inclination (Figures 11D, E).

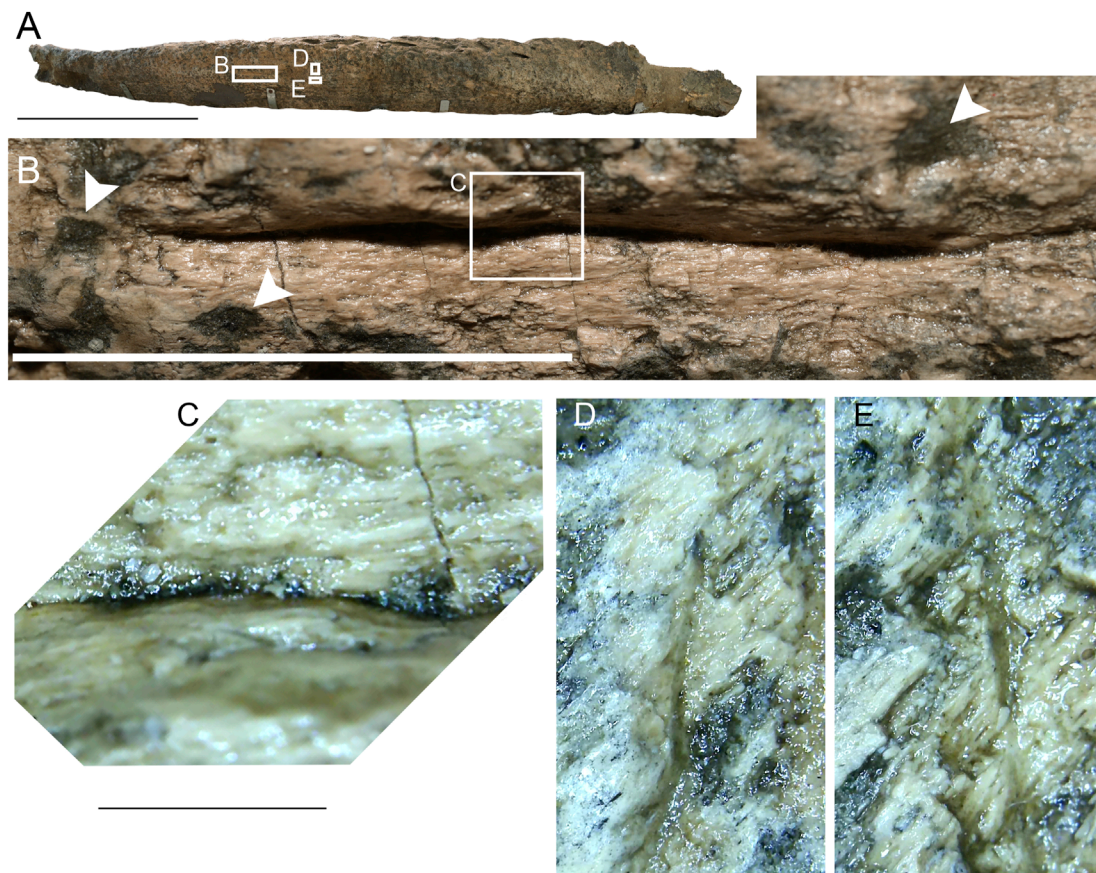


FIGURE 5
Opportunistic stage of the whale fall associated to MuMAB 240505. (A), left mandibular ramus showing the portions that are highlighted in the subsequent boxes. (B), highly magnificated type VI shark bite trace (scale bar equals 5 cm) with borings assigned to *Trypanites* sp. (C), digital microscopy of (B). (D), digital microscopy of anterior type I shark bite trace. (E), digital microscopy of posterior type I shark bite trace. Scale bars for (C, D) and E equal 1 cm. Pictures by MB published on permission of SABAP-PR PC.

4.2 Taphonomy of MuMAB 240506

4.2.1 Preservation and distribution of the bones

A total of 38 bones is present in the skeleton of [Figures 12A, B](#) representing about 20.3% of the total predicted bones in a generalized balaenopterid skeleton ([Supplementary Figure S1](#)). Therefore, only about one-fifth of the skeleton is preserved in this specimen. Even in this case, the presence of both mandibular rami and part of a forelimb supports the view that the specimen did not undergo prolonged floating after death.

The partial skeleton is almost completely disarticulated ([Figure 12](#)) as only 11 of the predicted 152 articulations are preserved (7.23%). Only parts of rostrum, basicranium, the posterior portions of both mandibular rami and a sequence of three cervical vertebrae are articulated. The preserved portions of the skull include a part of the rostrum in which premaxillae and maxillae are articulated, several fragments of the maxillae and premaxillae distributed within an area occupied by the anterior portion of the skeleton, the articulated basicranium (including parts of both squamosals, basioccipital and basisphenoid), and both the tympanoperiotic complexes detached from the remaining of the skull ([Figure 12](#)). The posterior portions of both the mandibular

rami are articulated with the corresponding squamosals. The left mandibular ramus is broken slightly posteriorly to the inferred position of the coronoid process; the right mandibular ramus lacks the dorsal-most part due to post-mortem processes and it is broken about 60 cm from the mandibular condyle. The right scapula is completely preserved in medial view. Three post-C₂ cervical vertebrae are articulated ([Figure 13](#)). Most of the vertebral epiphyses are detached and separated from the corresponding vertebral centra. The neural and left transverse processes of the thoracic vertebrae are broken suggesting some transportation of the bones. The preserved skeletal parts are located close to their original position in the living animal providing support to the hypothesis that the displacement was limited. It appears evident that the skeleton was dismembered and disarticulated before the completion of the decomposition of the tendons and muscles of the carcass. The burial occurred before the complete decay of the individual but after its massive disarticulation. Overall, most of the bones show a rough surface suggesting that the bones were exposed to external factors including bioturbation that altered the surface morphology.

There is no evidence of crushing on the skeleton: transverse fractures are not observed, while longitudinal fractures occur sparsely on the ribs.

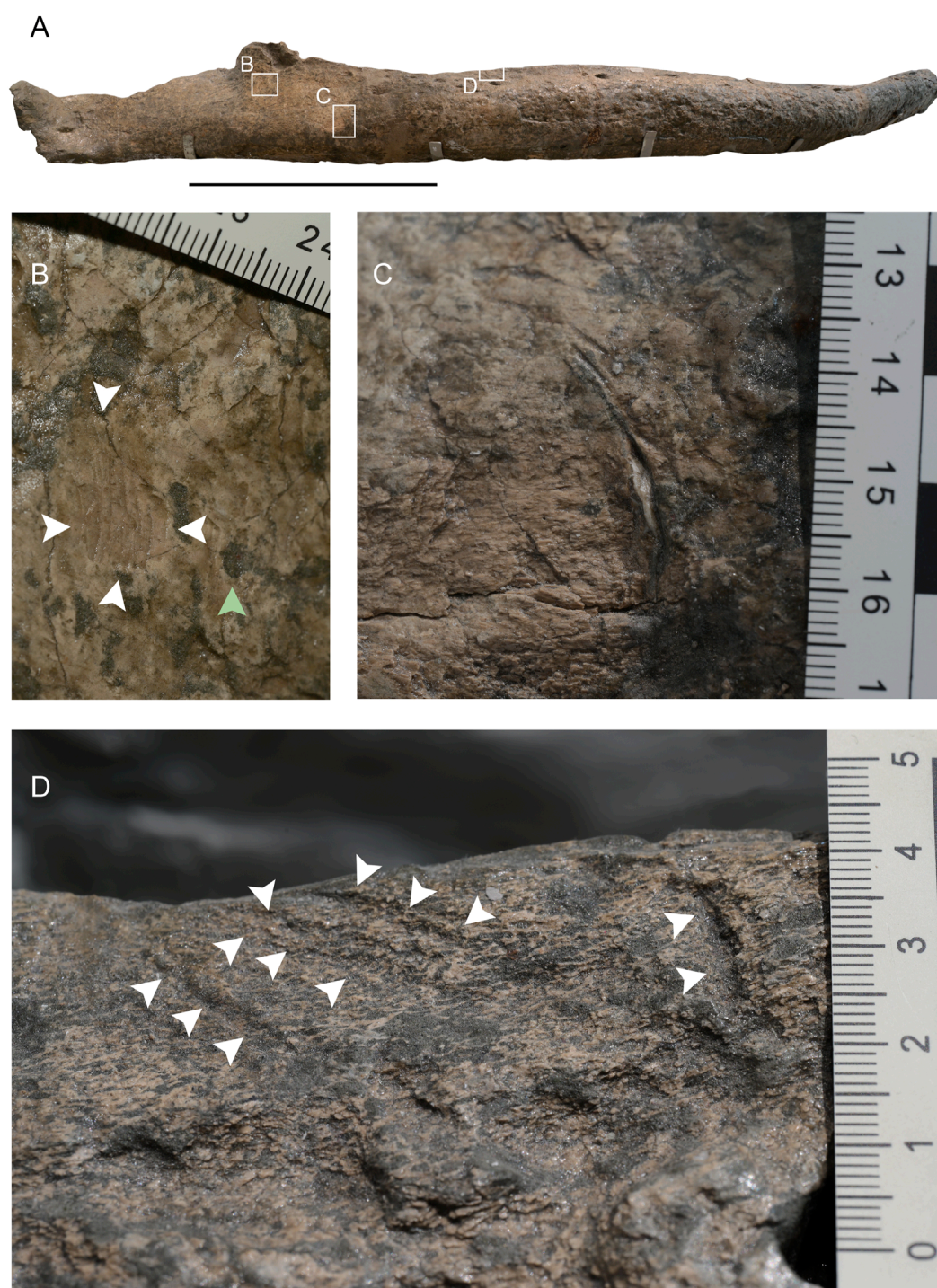


FIGURE 6

Opportunistic stage of the whale fall associated to MuMAB 240505. (A), right mandibular ramus showing the portions that are highlighted in the subsequent boxes. (B), feeding trace identified by four arrowheads; additional arrowheads indicate other feeding traces. (C), possible type VI shark bite trace. (D), scars attributed to shark bites. Pictures by MB published on permission of SABAP-PR PC.

4.2.2 Whale-fall analysis: opportunistic stage

Numerous borings are observed on the exposed surface of the scapula, on the vertebral bodies and on the vertebral epiphyses (Figure 12). In most cases, the borings are <10 mm in maximum width but some wider borings are

observed in the scapula where they show an elliptical outline.

Signs of opportunistic feeders are observed in some parts of the skeleton. Type I shark bite traces are seen on the marginal area of a vertebral epiphysis (Figures 13B, C).

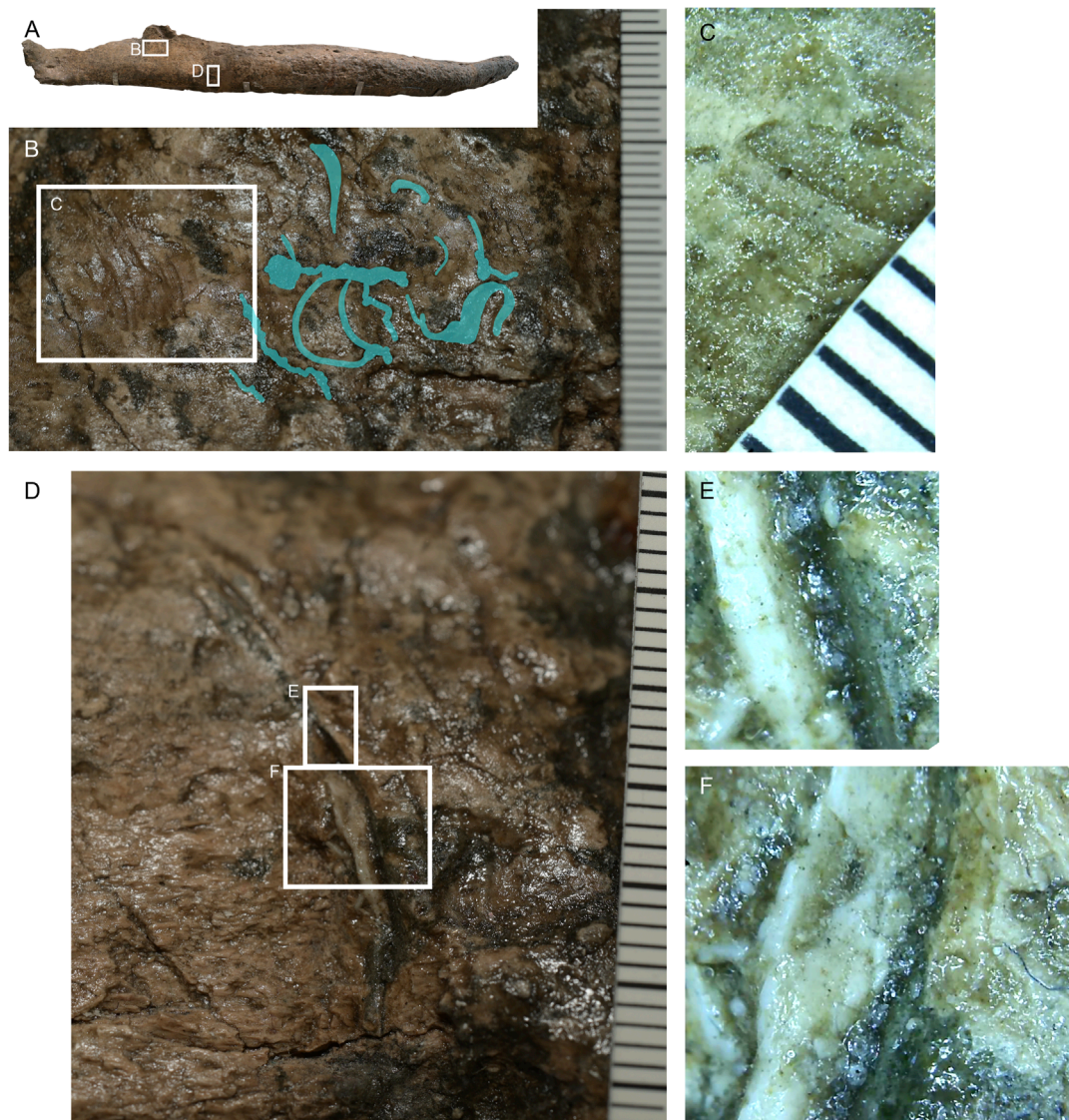


FIGURE 7

Opportunistic stage of the whale fall associated to MuMAB 240505. (A), right mandibular ramus showing the portions that are highlighted in the subsequent boxes. (B), indetermined feeding trace and possible *Meandropolydora* sp. feeding trace evidenced in blue-green. (C), digital microscopy of the indetermined feeding trace (scale in mm). (D), possible type VI shark bite trace showing portions that are highlighted in the subsequent boxes. (E,F), highly magnified parts of the shark bite trace in D. Scale of F and G as that in C. Pictures by MB published on permission of SABAP-PR PC.

A long and shallow channel (terminology according to Pirrone et al., 2014) is observed slightly close to the external border of a vertebral epiphysis located at the posterior end of the skeleton. The maximum width of this channel is about 10 mm and the channel is parallel to the external border of the epiphysis (Figures 13F, G). It is interpreted as a feeding trace of an invertebrate.

4.2.3 Reef stage

Numerous mollusc shells are observed on and between the bones (Figure 14A). A large fragment of *Atrina* sp. is located under the posterior portion of the left mandibular ramus (Figure 14B). A relatively large-sized shell of *Polinices* sp. is located between mandibular rami (Figure 14C), between the acetabular cavity of the scapula and the proximal head of one of the ribs; some

specimens of *Bolma speciosa* (Figures 14F,G) and one of *Tectonatica* sp. (Figure 14I) are located close to the dorsal surface of one of the vertebrae in the central portion of the skeleton. Scattered in the sediment are remains of *Conus puschi* and *Anadara* sp.; bivalve shells with still articulated valves referable to the families Arcidae and Veneridae are also visible in section. A pectinid bivalve is located amidst the posterior vertebrae (Figure 14D) and another to the dorsal surface of one of the vertebrae in the central portion of the skeleton (Figure 14E). A single spine of a cidaroid sea urchin is observed close to one of the vertebral centra (Figure 14H). The distribution of these specimens may have depended upon transportation.

In addition, a bivalve mollusc is found on the rib beneath the fourth cervical vertebra, a gastropod is placed on the neural



FIGURE 8

Opportunistic stage of the whale fall associated to MuMAB 240505. **(A)**, right maxilla showing the portions that are highlighted in the subsequent boxes. **(B)**, *Gastrochaenolithes* collapsed borings located along the maxillary margin. **(C)**, *Gastrochaenolithes* and *Trypanites* borings in close proximity to the lateral margin of the maxilla. **(D)**, mm-sized borings tentatively assigned to an *Osedax*-like bone-eating worm. **(E)**, left maxilla showing the portions that are highlighted in the subsequent boxes. **(F)**, multiple borings located on the premaxillae and maxillae in dorsal view which are assigned to *Gastrochaenolithes* and *Trypanites*. **(G)**, perforation pattern made up by *Gastrochaenolithes* and *Trypanites* along the lateral margin of the left maxilla. **(H)**, a large fragment of an indetermined ostreid located on the lateral process of the left maxilla. **(I)**, large *Gastrochaenolithes* borings on the dorsal surface of the left maxilla in close proximity to an indeterminate ostreid fragment documenting the reef stage. Pictures by MB published on permission of SABAP-PR PC.

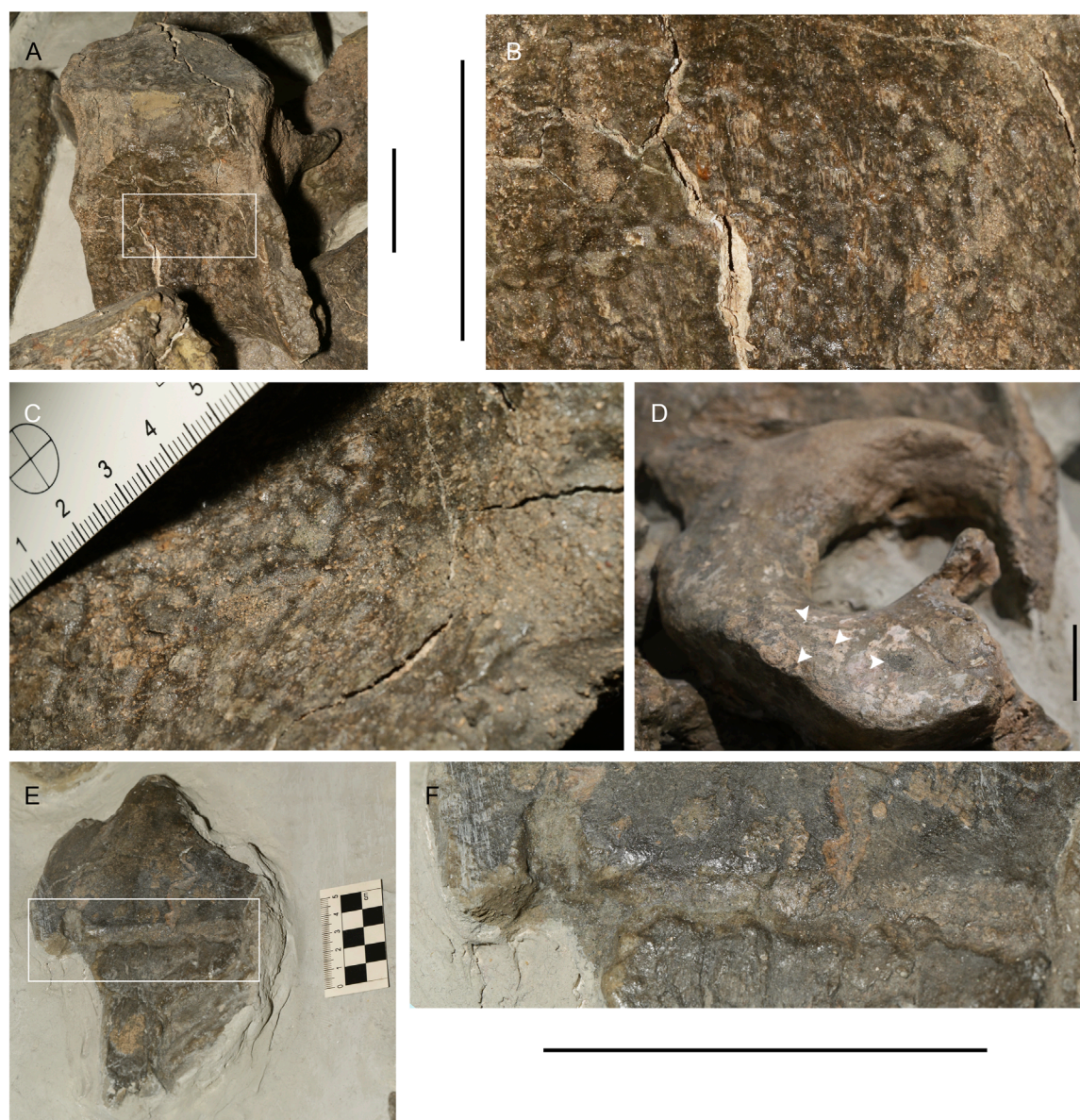


FIGURE 9

Opportunistic stage of the whale fall associated to the postcranial skeleton of MuMAB 240505. **(A)**, lumbar vertebra with indicated a box magnified in **B** (scale bar equals 5 cm). **(B)**, magnified area of **A** showing cm-sized borings (scale bar equals 5 cm). **(C)**, borings on the shaft of the radius. **(D)**, atlas with indications of multiple *Trypanites* borings tentatively attributed to *Osedax*-like bone-eating worms. **(E)**, indeterminate skull fragment with long sulcus magnified in **F**. **(F)**, magnified area shown in **E** illustrating the long sulcus that is supposed to represent an invertebrate feeding trace (scale bar equals 5 cm). Pictures by MB published on permission of SABAP-PR PC.

process of one of the posterior vertebrae, another bivalve appears to encrust another posterior vertebra and yet another bivalve shell encrusts the posterior-most neural process. These specimens are closely associated to the bones, and, in some cases, can be regarded as closely related to the bones themselves suggesting that the skeleton acted as hard substrate in which they lived. These shells show that the whale carcass underwent a reef stage and confirm that the skeleton remained exposed on the sea floor for a long time.

4.2.4 Post-depositional processes

Fractures developed transversely with respect to the longitudinal axis of the bone are observed in both mandibular rami but all the other skeletal portions, to the exclusion of the skull, do not show significant fractures. The absence of this kind of fractures together with the observation that the superimposition of bones to each other does not influence their integrity, suggests that scarce sedimentary weight was applied over the bones after burial.

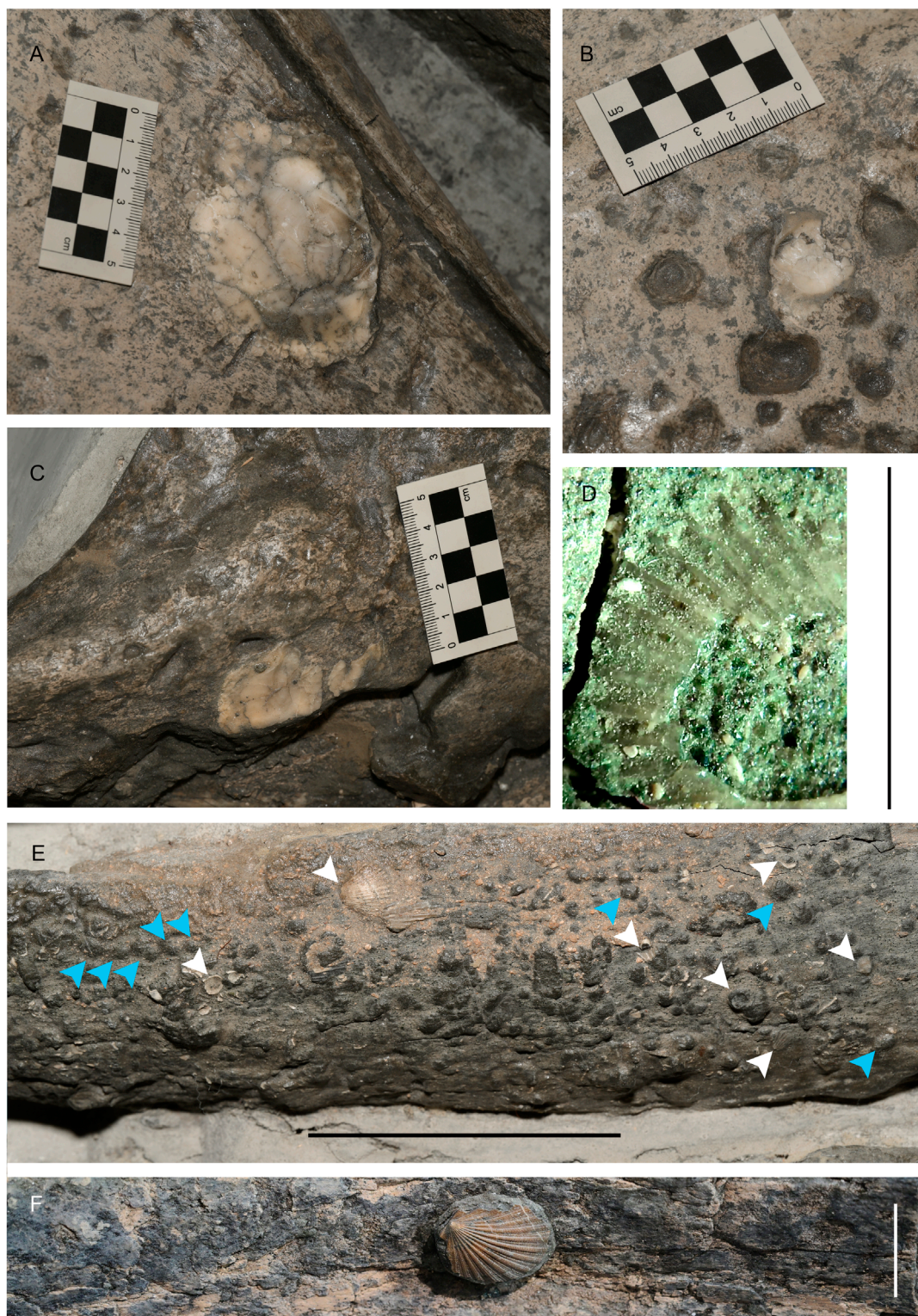


FIGURE 10
 Reef stage of the whale fall associated to MuMAB 240505. **(A)**, cemented valve of *Lophaflexa cf. plicatula* on the right maxilla. **(B)**, partial ostreid shell cemented on the right maxilla. **(C)**, partial ostreid shell cemented on the left lateral process of the maxilla. **(D)**, magnification of one of the molluscs present on the rib illustrated in **(D)** (scale bar equals 1 cm). **(E)**, rib surface with multiple indications of protruding sedimentary columns identified as fillings of borings perforating the bone (blue arrowheads) and molluscs (white arrowheads) (scale bar equals 10 cm). **(F)**, shell of *Chlamys cf. spinulosa* located on the medial surface of the left mandibular ramus and probably in life position (scale bar equals 5 cm). Pictures by MB published on permission of SABAP-PR PC.

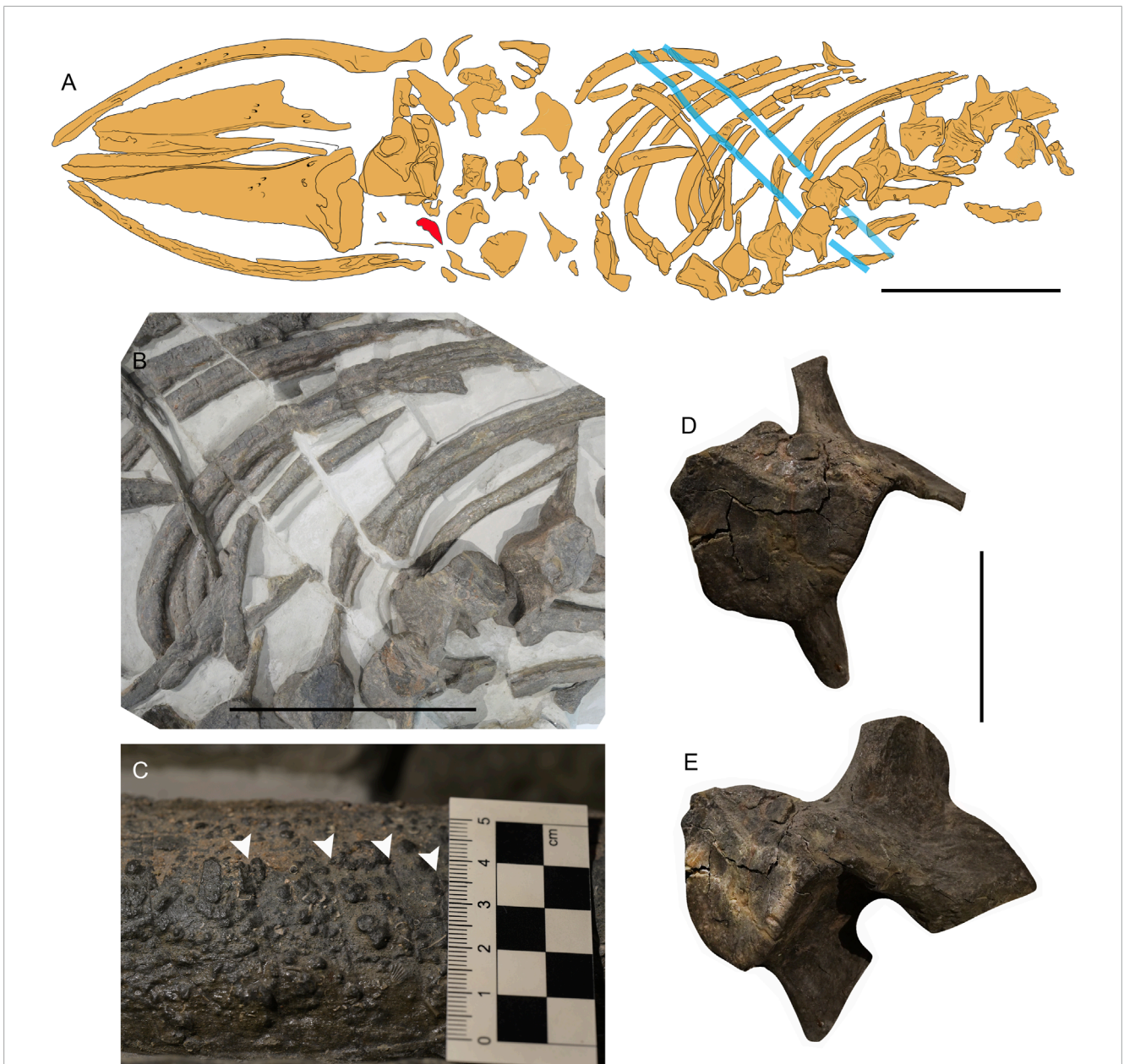


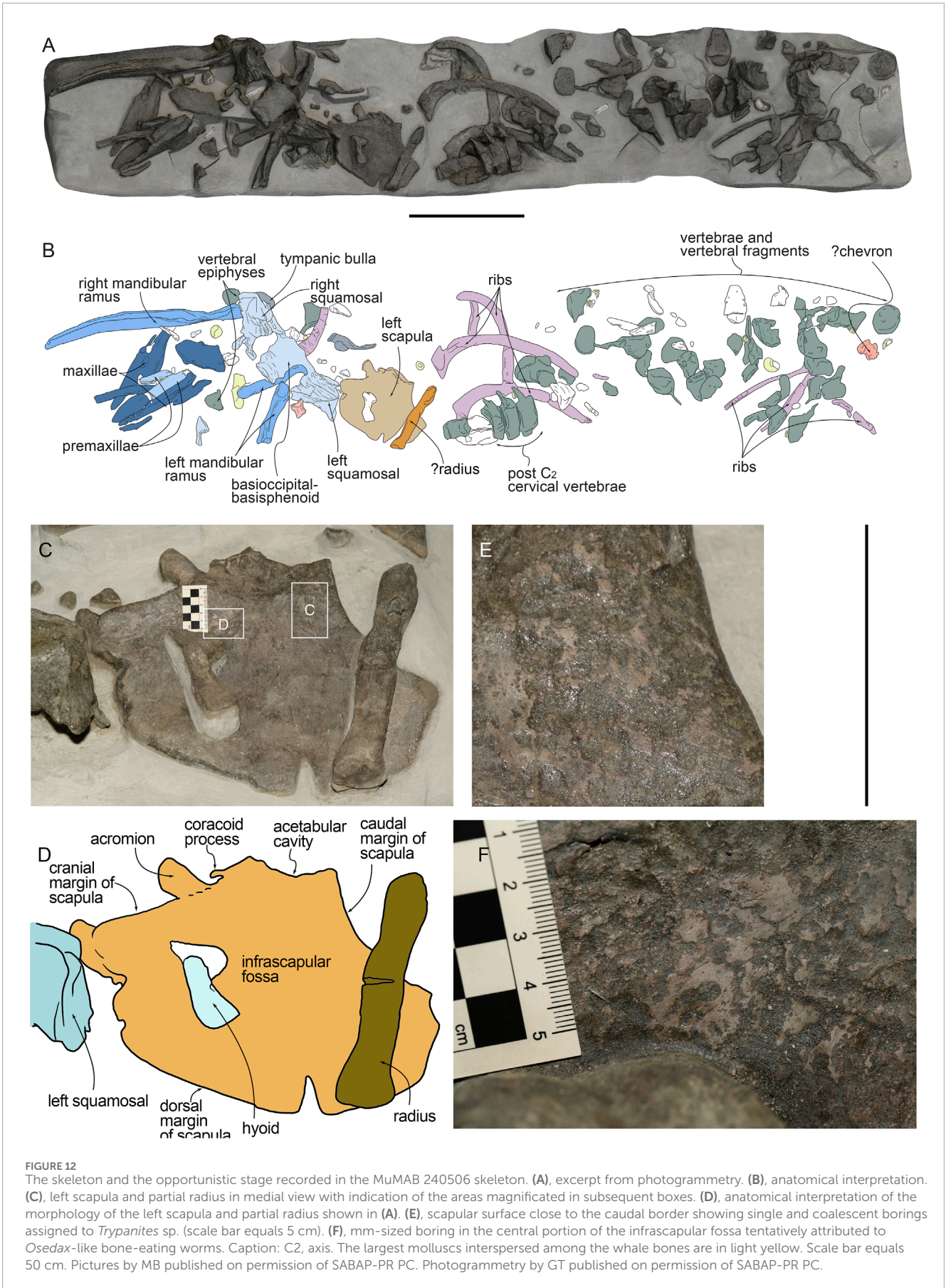
FIGURE 11

Evidences of post-depositional processes in the skeleton of MuMAB 240505, holotype of *Plesiobalaenoptera quarantellii*. (A), schematic representation of the skeleton showing two main faults (light blue lines) crossing the ribs and the lumbar vertebrae (scale bar equals 50 cm). (B), close-up view of the area of the ribcage where the main faults are located showing the fragmented ribs and the dislocations of some bony segments (scale bar equals 30 cm). (C), close-up view of one of the ribs showing micro-faults (arrowheads); the micro-faults are parallel to the main faults shown in (A, B). (D), deformed lumbar vertebra crossed by one of the main faults in anterior view. (E), deformed lumbar vertebra crossed by one of the main faults in anterolateral view. Scale bar for (C, D) equals 10 cm. Pictures by MB published on permission of SABAP-PR PC.

4.3 Taphonomy of the MuMAB 240508 periotic

The periotic was found among the bones of the holotype of *Plesiobalaenoptera quarantellii* but it was clear that it did not belong to that specimen because two additional tympanoperiotic complexes were found close to the corresponding articulation surfaces of the skull that presented the same morphologies (Bisconti, 2010; Bisconti et al., 2022).

In this periotic, the posterior process is absent but the other portions are well-preserved and do not show traces of exploitation by invertebrate or vertebrate saphrophagous animals (Figure 14). This observation is probably justified by the lack of significant amount of energy contained in the soft tissues of this portion and by the particularly hard material that constitutes it. In fact, the dorsal portion of the periotic is rugose and pachyosteosclerotic and this represents a significant obstacle to perforation and crushing. As far as periotic and bullae are concerned, none of the five periotics



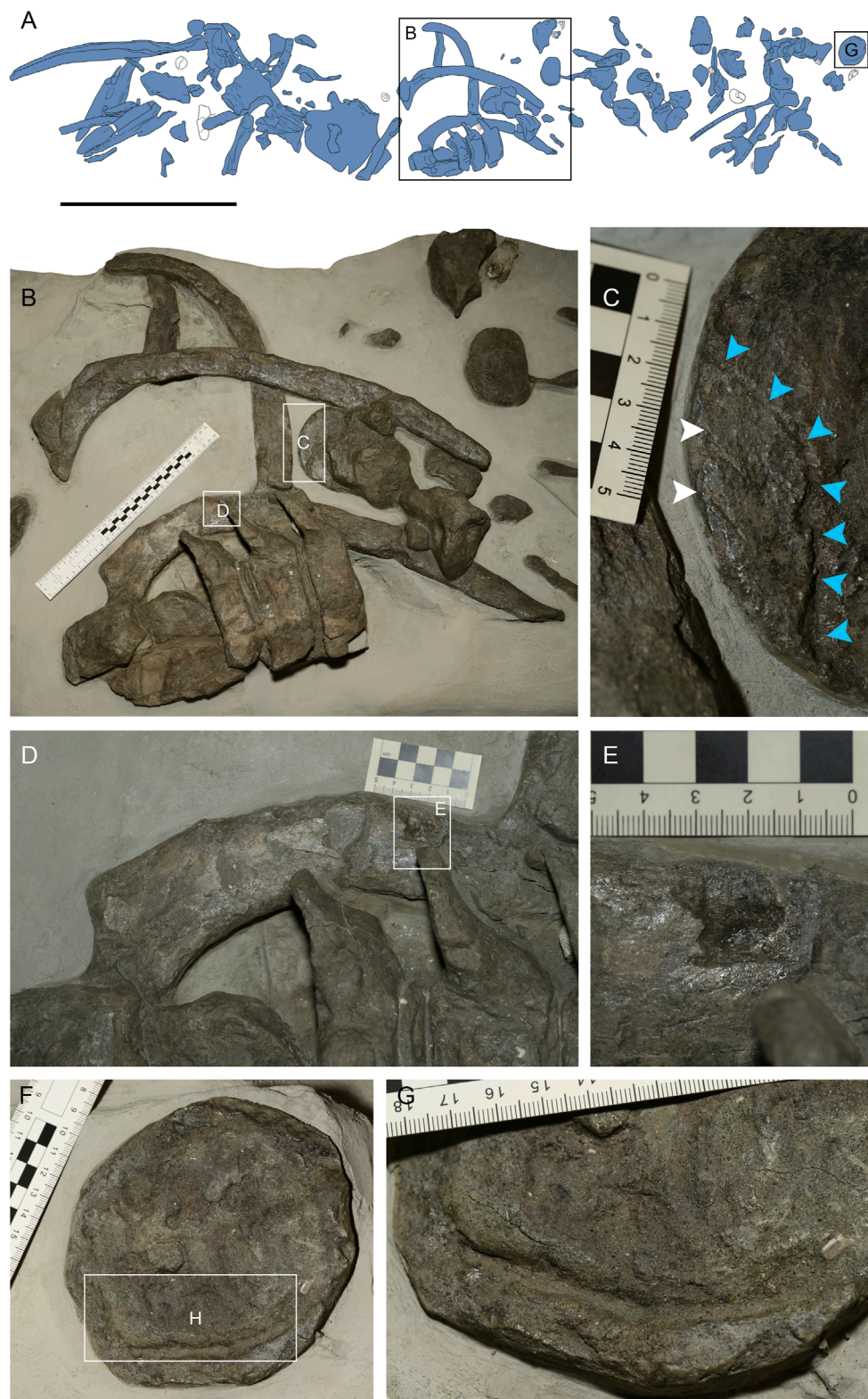


FIGURE 13

Opportunistic stage recorded in the MuMAB 240506 skeleton. **(A)**, scheme of the skeleton showing portions magnified in the subsequent boxes. **(B)**, portion including three cervical vertebrae, three almost complete ribs and other fragments including boxes subsequently magnified. **(C)**, magnified vertebral epiphysis showing two type I shark bite traces (white arrowheads) and a long sulcus attributed to an invertebrate feeding trace (blue arrowheads). **(D)**, rib with a circular boring compatible with a mammal bite trace. **(E)**, magnified portion of D showing the boring compatible with a mammal bite trace. **(F)**, vertebral epiphysis with curved sulcus. **(G)**, magnified portion of F showing the curved sulcus attributed to an invertebrate feeding trace. Pictures by MB published on permission of SABAP-PR PC.



FIGURE 14
 Reef stage recorded in the MuMAB 240506 skeleton and the MuMAB 240508 periotic. (A), scheme of the skeleton showing portions subsequently magnified. (B), a large specimen of *Atrina* sp. (C), large gastropod *Polinices* group located between the mandibular rami. (D), pectinid located in the posterior portion of the skeleton. (E), small bivalve located on a rib. (F), gastropod *Bolma speciosa* closely inserted in a natural concavity of the bones. (G), *Bolma speciosa*. (H), Cidaroid sea urchin spine. (I), large gastropod *Tectonatica* sp. The periotic MuMAB 240508 in (J), dorsal view; (K), medial view; (L), ventral view; (M), lateral view; scale bar equals 5 cm. Pictures by MB published on permission of SABAP-PR PC.

and four bullae preserved in the sample shows feeding traces of other signs of exploitation. The tympanoperiotic complexes may potentially represent the hard substrate for the development of the reef stage but, in the present case, this did not happen as there are no signs of mollusc or barnacle encrusting these bones.

The absence of the posterior process suggests that the periotic underwent violent breakage after it detached from the skull. Moreover, its location amidst the skeleton of *Plesiobalaenoptera quarantellii* suggests that it was displaced there from another specimen (currently not found). Given the absence of signs of traumatic impacts, we conclude that the transportation was short.

4.4 Systematic paleoichnology

4.4.1 *Trypanites* Mägdefrau, 1932

Trypanites isp.

Materials. Holotype skeleton of *Plesiobalaenoptera quarantellii*; skeleton MuMAB 240506. **Description.** A huge number of mm-sized, roundish openings is observed on the surface of the rostrum of *P. quarantellii*. These are illustrated in [Figures 8C,G–I](#). The openings are scattered along the bones and are variously spaced. In the ribs of *P. quarantellii*, we observe that the fillings of the channels possibly leading to *Trypanites* traces protrude out from the bone surface ([Figure 10D](#)).

In the skeleton MuMAB 240506, *Trypanites* traces are observed on the medial surface of the scapula ([Figure 12F](#)).

4.4.2 *Gnathichnus* Bromley, 1975

Gnathichnus isp.

Materials. Holotype skeleton of *Plesiobalaenoptera quarantellii*. **Description.** A single, star-like pattern observed in the left mandibular ramus slightly below the base of the coronoid process ([Figure 4D](#)). The pattern is formed by several crosses and star-like sulci on the surface of the bone that are reminiscent of a generalized *Gnathichnus* pattern following [Breton et al. \(1992\)](#). The whole pattern occupies a surface that is 20 mm in length and about 25 mm in height.

4.4.3 *Gastrochaenolithes* Leymerie, 1842

Gastrochaenolithes isp.

Materials. Holotype skeleton of *Plesiobalaenoptera quarantellii*. **Description.** Large, oval depressions excavating the bone are observed at several locations in the rostrum of *P. quarantellii* as documented in [Figures 8B,D,E,G,I](#); [Figure 10B](#) (see also [Supplementary Model S1](#)). The depressions are cm-sized and show vertical to converging lateral walls. Near the border of the rostrum, many depressions coalesce forming a long and wide bioerosional trace in which single depressions are often still distinguishable.

4.4.4 cf. *Meandropolydora* Voigt, 1965

cf. *Meandropolydora* isp.

Materials. Holotype skeleton of *Plesiobalaenoptera quarantellii*. **Description.** A single spot of meandering sulci compatible with cf. *Meandropolydora* isp. Following [Ruggiero and Bittner \(2008\)](#) is observed on the lateral surface of the right mandibular ramus of *P. quarantellii* ([Figure 7B](#)). The trace covers an area of about 20 mm in

height and 30 mm in length and includes a possible hole associated to a sinuous excavation that is tangential to the surface of the bone.

5 Discussion

Associations of invertebrate species and vertebrate bones are known from the marine sedimentary record since the Jurassic with examples from ichthyosaurs, plesiosaurs and chelonians ([Jamison-Todd et al., 2023](#); [Danise et al., 2014](#); [Kiel et al., 2009](#)). The fossil evidence of these associations includes traces interpreted as feeding signs made by echinoids on microbial mat covering the exposed bones at a certain point, microborings attributed to cyanobacteria and feeding traces assigned to *Radulichnus*, *Gnathichnus*, *Meandropolydora*, *Entobia*, *Trypanites*, *Gastrochaenolithes* and others ([Table 1](#)). These traces suggest that a diverse assemblage of invertebrate species exploited the corresponding carcasses including sea urchins, crabs, gastropods, sponges and so on. Another recently-described case study involved a couple of large-sized plesiosaurs in which chemoautotrophic mollusc species were found together with extensive microboring perforations attributed to bone-penetrating bacteria ([Kaim et al., 2008](#)), as those described by [Deming et al. \(1997\)](#) in modern whale-falls. In the first plesiosaur carcass, both the opportunistic and reef stages are documented, and in the second carcass, apart from these two stages, also the chemoautotrophic stage is found.

Whale falls from the early Cenozoic include several cases described by [Kiel et al. \(2009\)](#), [Kiel and Goedert \(2006\)](#) and [Goedert et al. \(1995\)](#). In all these cases chemoautotrophic molluscs were found in close association to the whale bones discovered in Eocene and Oligocene sediments in North America representing bathyal communities. In certain cases, it was suggested that the whale bones remained on the sea floor for about 1,000 years before being buried ([Kiel et al., 2009](#)).

Most Miocene whale-falls are from sediments representing deep sea contexts. [Jenkins et al. \(2018\)](#), [Amano and Kiel \(2014\)](#) and [Amano and Little \(2005\)](#), described mollusc associations found in close proximity to whale bones from different locations and discovered that chemoautotrophic molluscs were normally present. Only a few Miocene whale-falls actually represent shallow marine conditions; these include cases from Argentina ([Farroni et al., 2024; 2022](#)) in which the presence of barnacles is associated to abrasion, moderate corrosion, encrustation and lack of bioerosion, suggesting deposition of the whale carcass on a soft bottom. A similar case is known from Spain ([Belaústegui et al., 2011](#)).

In a single Pleistocene whale fall, [Seki and Jenkins \(2021\)](#) documented shallow sea depth and absence of chemoautotrophic mollusc species; [Farroni et al. \(2024\)](#), [Farroni et al. \(2022\)](#) confirmed the absence of chemoautotrophic molluscs in the Argentinean, shallow water, Miocene whale-falls. Apparently, according to [Farroni et al. \(2024\)](#), [Farroni et al. \(2022\)](#), the presence of a chemoautotrophic community is strictly related to sea depth.

The three balaenopterid carcasses studied in the present paper add new important information about the whale fall patterning during the Miocene. We observe three different biostratigraphic histories able to explain the peculiar bone distributions of these specimens. First, in the case of the holotype of *Plesiobalaenoptera*

TABLE 1 Observations on whale falls and whale fall-like communities beginning from the Jurassic.

Age	Taxa	Observed whalefall and whale fall-like stages	Water depth	Traces on the bones	Refs
Jurassic onward	ichthyosaurs chelonians plesiosaurs	opportunistic reef chemoautothrophic		<i>Radulichnus</i> <i>Gnaticmus</i> <i>Meandropolydora</i> <i>Entobia</i> <i>Trypanites</i> <i>Gastrochaenolithes</i>	Danise et al. (2014), Kaim et al. (2008), Kiel et al. (2009), Jamison-Todd et al. (2023), Heijne et al. (2019)
Eocene, Oligocene	whales	chemoautothrophic	batyhyal		Goedert et al. (1995), Kiel and Goedert (2006), Kiel et al. (2010b)
Miocene	whales	chemoautothrophic	batyhyal		Amano and Little (2005), Amano (2006), Amano and Kiel (2014), Farroni et al. (2022), Farroni et al. (2024), Jenkins et al. (2018), Pyenson and Haasl (2007)
	whales	opportunistic reef	shallow	abrasion, moderate corrosion, encrustation	
Pliocene	whales	chemoautothrophic	deep		Dominici et al. (2009), Dominici et al. (2020), Higgs et al. (2012), Bisconti et al. (2021a)
	whales	scarce-to-no chemoautothroph	shallow		
	whales	scarce trace related to <i>Osedax</i> -like taxa	deep + shallow (Piedmont basin)	abrasion, moderate corrosion, encrustation, bioerosion	

quarantellii, we found an ichnofossil association with presence of *Trypanites* that is related to hardgrounds characterized by scarce-to-null sedimentation (e.g., Vinn and Toom, 2016; Brett and Liddell, 1978); sedimentary starvation is also known in contexts rich in glauconite like that of this balaenopterid. Tectonic activity is normally associated to hardground formation (e.g., Gale, 2019) corroborating the pattern observed on this whale in which tectonic activity appears pervasive. In this case, the trace fossil association together with a well-documented reef stage support the view that the animal was not transported far from the site of the deposition on the sea floor and remained exposed for a long amount of time providing hard substrate for mollusc encrustation. These data and the absence of an enveloping crust on the whale skeleton support the hypothesis that it was decomposed and remained on the seafloor in well-oxygenated waters.

Specimen MuMAB 240508 shows a different biostratinomic history characterized by an intense breakage of the bones, scarce reef stage and less developed trace fossil assemblage. Interestingly, the molluscs associated with this skeleton are mainly vagile epifaunal gastropods and infaunal bivalves that are not in life position. Some of the observed species preferentially live at shallower depths. Both the skeletal preservation and the characteristics of the mollusc association suggest that both the carcass and the molluscs were transported from a location characterized by shallower water implying that the disarticulation of the skeleton was not

complete, therefore the anteroposterior axis of the skeleton was preserved.

The third specimen, MuMAB 240506, is represented by a single partial bone that moved from the original skeleton after disarticulation. None is known about the original skeleton. The specimen is broken suggesting violent displacement. It is represented by a tympanoperiotic complex that may potentially represent the hard substrate for the development of a reef stage but, in the present case, this did not happen as there are no signs of mollusc or barnacle encrusting these bones.

We thus document different processes acting in the Upper Tortonian of the Padan Gulf of northern Italy in the same sedimentary basin. This observation suggests that preservation styles of whale carcasses may depend on different biostratinomic processes even at local scales that may be considered substantially unrelated to sedimentation rates. Our results are in broad accordance with those provided by Bisconti et al. (2021a) that showed different patterns of preservation in a baleen whale assemblage from the Sabbie d'Asti Formation in northern Italy (Piedmont) and with those presented by Heijne et al. (2019) about the taphonomy of plesiosaurs from the Middle Triassic of Winterswijk (Holland) that cannot be explained by a single biostratinomic model.

Our observations on the preservation of the specimens studied herein, together with the description of the preservation of the Orciano Pisano whale made by Dominici et al. (2009), show that the

thoracic region of the vertebral column is absent; this observation is consistent with an analysis of a modern whale fall studied on a bathyal sea floor near to Vancouver Island (Canada) where a large gap is recorded between the skull and the caudal vertebrae; this gap is interpreted as the result of a higher degradation rate of the thoracic and lumbar regions of the whale body (Lundsten et al., 2010a). Moreover, in their analysis of six extant whale falls communities of the Monterey Canyon, Lundsten et al. (2010b) reported that in all cases the thoracic region of the whale body was the one that was destroyed first. It is reasonable to suppose that the central portions of the cetacean body represent a more voluminous energy reservoir that is exploited first by the decomposing communities. Interestingly, this pattern occurs independently from the depth of the floor where the whale carcass is deposited as it is observed in the present-day abyssal whale falls as well as in Pliocene and Miocene shallow water whale falls.

A number of case studies from the Pliocene fossil record have been reported in recent literature about whale falls. Dominici et al. (2009) analyzed numerous whale falls from the Pliocene record of Italy and concluded that carcasses deposited at lower depths (they called these examples shelf whale-falls) show lower probability to host specialized, chemoautotrophic molluscan communities. The latter are mostly present below the shelf break confirming the suggestion that the depth of the carcass deposition site is the principal determinant of the taxonomic and ecologic composition of the whale fall community. Our work apparently confirms this suggestion as the carcasses studied here are from a Tortonian marine fall whose depth is estimated in about 100 m based on molluscs and fish otoliths.

Further works published by Bisconti et al. (2023a), Bisconti et al. (2021a), Bisconti et al. (2021b) showed that whale skeletons deposited in clayey or sandy floors in Piedmont and Emilia Romagna do not show signs of chemoautotrophic molluscs whereas they show presence of *Osedax*-like borings, shark bite traces, feeding traces of other invertebrates and well documented reef stages in several cases. Additional work is currently in progress about the whale fall record from an Early Pliocene balaenopterid from southern Tuscany (Bisconti et al., 2023b; Scotton et al., 2020; 2018). Differing from Miocene whale falls documented in the Pacific Ocean, in Mediterranean only a few cases show presence of chemoautotrophic molluscan species whereas reef stages are mainly recorded in the Mediterranean Pliocene and Miocene fossil record but not in deep sea whale falls from both present and during Miocene times.

The evidence at hand does not allow to observe a linear evolutionary pattern for whale fall communities. Cases suggesting similarities between whale and wood falls are well documented (e.g., Glover et al., 2013; Kiel et al., 2010a; Kiel and Goedert, 2006) and cases suggesting the possibility that chemoautotrophic molluscs opportunistically moved from seep environments to whale carcasses are described (Amano, 2006). Differences between shelf and deep sea whale falls are now clear based on studies on both modern and fossil records. However, despite this amount of data, it is still difficult to discern the evolutionary steps leading to the different taxonomic compositions and ecological networks of shelf and deep-sea whale fall communities. Moreover, the discovery of a whale-fall developed around a small-sized mysticete from the Miocene of California (Pyenson and Haasl, 2007) and the finding that *Osedax*-like worms

can exploit the carcasses of marine birds (Kiel et al., 2010b) clearly show that the enormous amount of energy represented by the large baleen whale carcasses does not constitute a prerequisite for the origin and evolution of decaying specialized communities.

We observed that the origin and evolution of whale-fall communities was a complex process involving opportunistic behaviors by species inhabiting the sea floors where the carcasses were deposited. While our data corroborates the previously documented absence of chemoautotrophic molluscs at shallow whale-falls, chemoautotrophic organisms are present in anoxic environments that are rich in sulphates and sulphurs, or sulphides (Treude et al., 2009). This better explains the association between chemoautotrophic molluscs and decaying whale carcasses which may lead to local depletion of Oxygen (e.g., Treude et al., 2009; Braby et al., 2007). Shallow water conditions with high instability in sedimentary supply may still maintain high Oxygen levels during the decomposition processes, preventing the formation of methane. This may represent a physiological explanation for the absence of chemoautotrophic molluscs in shallow whale falls.

Additional investigation is necessary to test a hypothesis that chemoautotrophic species occur in whale falls only in the cases in which seep ecosystems are located within a distance range from the whale falls. We also suggest that *Osedax*-like larvae may be more widespread than expected being able to settle vertebrate carcasses wherever present independently from the size of the hosting dead body. Finally, we do not find specific differences in the biostratigraphic processes occurring at the La Bocca site with respect to modern whale-falls from abyssal floors with respect to the distribution of the bones of the whales after years of permanence on the floor before burial.

6 Conclusion

We studied the taphonomy of three balaenopterid specimens from the Tortonian of La Bocca area at the Scipione Ponte Locality near Salsomaggiore Terme, northern Italy. The specimens included two associated, partial skeletons and a single periotic. The skeletons are disturbed and show dense traces documenting intense bioerosion by sharks and a wealth of invertebrates suggesting their permanence on the sea floor for several, perhaps hundreds of years. The paleoecological analysis of the site including microfossils, molluscs and fish otoliths supports the inference that the paleodepth of the site was around 100 m. The intense bioturbation allows to infer the settlement of the opportunistic and reef stages on these carcasses with large impact of sharks and invertebrate feeding traces. The sedimentological evidences help to explain the distribution of the bones and the range of disarticulation observed in the specimens. The present work contributes to the ongoing debate on the origin and evolution of whale fall communities by confirming a relationship between water depth and presence of chemosynthetic molluscan species, by showing presence of a range of borings in part compatible with *Osedax*-like worms and in part compatible with the ichnogenera *Gastrochaenolites*, *Meandropolydora* and *Trypanites*, thereby suggesting that the carcasses were intensely exploited by a complex community.

Data availability statement

The original contributions presented in the study are included in the article/[Supplementary Material](#), further inquiries can be directed to the corresponding author.

Ethics statement

Ethical approval was not required for the study involving animals in accordance with the local legislation and institutional requirements because The samples are from fossil specimens. Written informed consent was not obtained from the individual(s) for the publication of any potentially identifiable images or data included in this article because the images are from historical records in the Municipality of Salsomaggiore Terme.

Author contributions

MB: Formal Analysis, Investigation, Methodology, Supervision, Validation, Writing – original draft, Writing – review and editing. PM: Formal Analysis, Investigation, Methodology, Supervision, Validation, Writing – original draft, Writing – review and editing. GR: Data curation, Formal Analysis, Investigation, Methodology, Resources, Visualization, Writing – original draft, Writing – review and editing. GT: Methodology, Software, Visualization, Writing – review and editing. GC: Formal Analysis, Investigation, Methodology, Supervision, Validation, Writing – original draft, Writing – review and editing.

Funding

The author(s) declare that no financial support was received for the research and/or publication of this article.

Acknowledgments

The authors wish to remember the fundamental contribution made by the late Raffaele Quarantelli to the discovery, excavation, preparation and exhibition of the three specimens discussed in the present paper. His enthusiasm, devotion and hard work will never be forgotten by those who knew him working on the fossil skeletons. Many thanks are due to Francesca Vallé and to SABAP-PR PC who

References

- Alfaro-Lucas, J. M., Shimabukuro, M., Ferreira, G. D., Kitazato, H., Fujiwara, Y., and Sumida, P. Y. G. (2017). Bone-eating *Osedax* worms (Annelida: siboglinidae) regulate biodiversity of deep-sea whale-fall communities. *Deep-Sea Res. II* 146, 4–12. doi:10.1016/j.dsr2.2017.04.011
- Allison, P. A., Smith, C. R., Kukert, H., Deming, J. W., and Bennett, B. A. (1991). Deep-water taphonomy of vertebrate carcasses: a whale skeleton in the bathyal Santa Catalina Basin. *Paleobiology* 17, 78–89. doi:10.1017/s0094837300010368

allowed the study of the specimens (authorization Prot. No. 12819, 11 November 2024).

Conflict of interest

The authors declare that the research was conducted in the absence of any commercial or financial relationships that could be construed as a potential conflict of interest.

Generative AI statement

The author(s) declare that no Generative AI was used in the creation of this manuscript.

Publisher's note

All claims expressed in this article are solely those of the authors and do not necessarily represent those of their affiliated organizations, or those of the publisher, the editors and the reviewers. Any product that may be evaluated in this article, or claim that may be made by its manufacturer, is not guaranteed or endorsed by the publisher.

Supplementary material

The Supplementary Material for this article can be found online at: <https://www.frontiersin.org/articles/10.3389/feart.2025.1558428/full#supplementary-material>

Supplementary Figure S1 |

Schemes illustrating generalized balaenopterid skeleton as from Bisconti et al. (2021) to show the preserved portions of the two balaenopterid skeletons analyzed in this paper. Red rectangles represent preserved portions. (A) MuMAB 240505. (B) MuMAB 240506. c, carpal; c1-c7, cervical vertebrae 1-7; Cd1-Cd23, caudal vertebrae 1-23; che 1-12, chevrons 1-12; d1 and d2, left and right dentaries; ear tp1 and ear tp2, left and right tympanoperiotic complexes; i1-3, stylohyoids and tyrohyoid; h, humerus; L1-L13, lumbar vertebrae 1-13; mc, metacarpal; ph, phalanx; p1 and p2, left and right pelvis; r, radius; rib1-28, ribs 1-28sc, scapula; sk, skull; st, sternum; T1-T14, thoracic vertebrae 1-14; u, ulna. Pictures by MB published on permission of Soprintendenza Archeologia Belle Arti e Paesaggio per le Province di Parma e Piacenza (SABAP-PR PC).

Supplementary Video S1 |

Three-dimensional model of the right maxilla of the holotype of *Plesiobalaenoptera quarantellii* (MuMAB 240505) showing trace fossils of different sizes.

- Amano, K. (2006). Recent and fossil whale-fall communities – with special remarks on molluscs. *Fossils – Palaeontol. Soc. Jpn.* 80, 5–16.

- Amano, K., and Kiel, S. (2014). Drill holes in bathymodiolin mussels from a Miocene whale-fall community in Hokkaido, Japan. *Veliger* 49, 265–269.

- Amano, K., and Little, C. T. S. (2005). Miocene whale-fall community from Hokkaido, northern Japan. *Palaeogeogr. Palaeoclim. Palaeoecol.* 215, 345–356. doi:10.1016/j.palaeo.2004.10.003

- Amorosi, A. (1997). Detecting compositional, spatial, and temporal attributes of glaucony: a tool for provenance research. *Sed. Geol.* 109, 135–153. doi:10.1016/s0037-0738(96)00042-5
- Artoni, A., Papani, G., Rizzini, F., Calderoni, M., Bernini, M., Argnani, A., et al. (2004). The Salsomaggiore structure (Northwestern Apennine foothills, Italy): a Messinian Mountain front shaped by mass-wasting products. *Geacta* 3, 107–127.
- Belaústegui, Z., de Gibert, J. M., Domènech, R., Muñiz, F., and Martinell, J. (2011). Tafonomía y contexto paleoambiental de los restos de un cetáceo del Mioceno medio de Tarragona (NE España). *Geobios* 44, 19–31. doi:10.1016/j.geobios.2010.07.002
- Bisconti, M. (2003). *Systematics, Palaeoecology, and palaeobiogeography of the archaic mysticetes from the Italian Neogene*. PhD tesi (Pisa: Università di Pisa), 344.
- Bisconti, M. (2006). *Titanocetus*, a new baleen whale from the middle Miocene of northern Italy (mammalia, cetacea, mysticeti). *J. Vert. Pal.* 26, 344–354. doi:10.1671/0272-4634(2006)26[344:tanbwf]2.0.co;2
- Bisconti, M. (2010). A new balaenopterid whale from the late Miocene of the Stirone River, northern Italy (mammalia, cetacea, mysticeti). *J. Vert. Pal.* 30, 943–958. doi:10.1080/02724631003762922
- Bisconti, M., Chicchi, S., Monegatti, P., Scacchetti, M., Campanini, R., Marsili, S., et al. (2023a). Taphonomy, osteology and functional morphology of a partially articulated skeleton of an archaic Pliocene right whale from Emilia Romagna (NW Italy). *Boll. Soc. Pal. It.* 62, 1–32. doi:10.4435/BSPI.2023.09
- Bisconti, M., Damarco, P., Mao, S., Pavia, M., and Carnevale, G. (2021c). The earliest baleen whale from the Mediterranean: large-scale implications of an early Miocene thalassotherian mysticete from Piedmont, Italy. *Pap. Palaeont.* 7, 1147–1166. doi:10.1002/spp2.1336
- Bisconti, M., Damarco, P., Marengo, L., Macagno, M., Daniello, R., Pavia, M., et al. (2024). Anatomy and relationships of a new gray whale from the Pliocene of Piedmont, northwestern Italy. *Diversity* 16, 547. doi:10.3390/d16090547
- Bisconti, M., Damarco, P., Pavia, M., Sorce, B., and Carnevale, G. (2021b). *Marzanoptera tersillae*, a new balaenopterid genus and species from the Pliocene of Piedmont, north-west Italy. *Zool. J. Linn. Soc.* 192, 1253–1292. doi:10.1093/zoolinnean/zlaa131
- Bisconti, M., Damarco, P., Santagati, P., Pavia, M., and Carnevale, G. (2021a). Taphonomic patterns in the fossil record of baleen whales from the Pliocene of Piedmont, north-west Italy (mammalia, cetacea, mysticeti). *Boll. Soc. Pal. It.* 60, 183–211. doi:10.4435/BSPI.2021.14
- Bisconti, M., Raineri, G., Tartarelli, G., Monegatti, P., and Carnevale, G. (2022). The periotic of a basal balaenopterid from theortonian of the Stirone River, northern Italy (cetacea, mysticeti, Balaenopteridae). *Palaeobiodivers. Palaeoenvir.* 103, 663–679. doi:10.1007/s12549-022-00550-2
- Bisconti, M., Scotton, R., Santagati, P., Foresi, L. M., Ragaini, L., Tartarelli, G., et al. (2023b). A whale in a vineyard: palaeontological preparation and education during the 'Brunella' Project, a large-scale conservation effort focused on a Pliocene whale in southern Tuscany. *Italy. Geohist.* 15, 1. doi:10.1007/s12371-022-00766-w
- Bisconti, M., and Varola, A. (2000). Functional hypothesis on an unusual mysticete dentary with double coronoid process from the Miocene of Apulia and its systematic and behavioural implications. *Palaeontogr. It.* 87, 19–35.
- Bisconti, M., and Varola, A. (2006). The oldest eschrichtiid mysticete and a new morphological diagnosis of Eschrichtiidae (Gray Whales). *Riv. It. Pal. Strat.* 112, 1–11. doi:10.13130/2039-4942/6352
- Boessenecker, R. W. (2013). A new marine vertebrate assemblage from the late Neogene purisima Formation in central California, part II: pinnipeds and cetaceans. *Geodiv* 35, 815–940. doi:10.5252/g2013n4a5
- Bosio, G., Collareta, A., Di Celma, C., Lambert, O., Marx, F. G., de Muizon, C., et al. (2021). Taphonomy of marine vertebrates of the Pisco Formation (Miocene, Peru): insights into the origin of an outstanding fossil-lagerstätte. *Plos One* 16, e0254395. doi:10.1371/journal.pone.0254395
- Braby, C. E., Rouse, G. W., Johnson, S. B., Jones, W. J., and Vrijenhoek, R. C. (2007). Bathymetric and temporal variation among *Osedax* boneworms and associated megafauna on whale-falls in Monterey Bay, California. *Deep-Sea Res. I* 54, 1773–1791. doi:10.1016/j.dsr.2007.05.014
- Breton, G., Neraudeau, D., and Cuenca-Boulat, C. (1992). *Gnathichnus stellarum* ichnosp. nov., trace broutage d'un échinide Camp. Charentes Fr. *Paléob.* 11, 219–229.
- Brett, C. E., and Liddell, W. D. (1978). Preservation and paleoecology of a Middle Ordovician hardground community. *Paleobiology* 4, 329–348. doi:10.1017/s0094837300006035
- Carlucci, R., Sassanelli, G., Matarrese, A., Giove, A., and D'Onghia, G. (2010). Experimental data on growth, mortality and reproduction of *Ostrea edulis* (L., 1758) in a semi-enclosed basin of the Mediterranean Sea. *Aquacult* 306, 167–176. doi:10.1016/j.aquaculture.2010.05.026
- Cigala Fulgosi, F. (1990). Predation (or possible scavenging) by a great white shark on an extinct species of bottlenosed dolphin in the Italian Pliocene. *Tert. Res.* 12, 17–36.
- Collareta, A., Lambert, O., Landini, W., Di Celma, C., Malinverno, E., Varas-Malca, R., et al. (2017). Did the giant extinct shark *Carcharocles megalodon* target small prey? Bite marks on marine mammal remains from the late Miocene of Peru. *Palaeogeogr. Palaeoclim. Palaeoecol.* 469, 84–91. doi:10.1016/j.palaeo.2017.01.001
- Cornacchia, I., Brandano, M., and Agostini, S. (2021). Miocene paleoceanographic evolution of the Mediterranean area and carbonate production changes: a review. *Earth-Sci. Rev.* 221, 103785. doi:10.1016/j.earscirev.2021.103785
- Dahlgren, T., Wiklund, H., Källström, B., Lundälv, T., Smith, C., and Glover, A. (2006). A shallow-water whale-fall experiment in the north Atlantic. *Cah. Biol. Mar.* 47, 385–389.
- Dahlgren, T. G., Glover, A. G., Baco, A., and Smith, C. R. (2004). Fauna of whale falls: systematics and ecology of a new polychaete (Annelida: chrysopetalidae) from the deep Pacific Ocean. *Deep Sea Res. I* 51, 1873–1887. doi:10.1016/j.dsr.2004.07.017
- Danise, S., Twitchett, R. J., and Matts, K. (2014). Ecological succession of a Jurassic shallow-water ichthyosaur fall. *Nat. Comm.* 5, 4789. doi:10.1038/ncomms5789
- Deming, J. W., Reysenbach, A. L., Macko, S. A., and Smith, C. R. (1997). Evidence for the microbial basis of a chemoautotrophic invertebrate community at a whale fall on the deep seafloor: bone-colonizing bacteria and invertebrate endosymbionts. *Microsc. Res. Tech.* 37, 162–170. doi:10.1002/(sici)1097-0029(19970415)37:2<162::aid-jemt4>3.0.co;2-q
- Dominici, S., Cioppi, E., Danise, S., Betocchi, U., Gallai, G., Tangocci, F., et al. (2009). Mediterranean fossil whale falls and the adaptation of mollusks to extreme habitats. *Geology* 37, 815–818. doi:10.1130/g30073a.1
- Dominici, S., Danise, S., Cau, S., and Freschi, A. (2020). The awkward record of fossil whales. *Earth-Sci. Rev.* 205, 103057. doi:10.1016/j.earscirev.2019.103057
- Farroni, N. D., Cuitiño, J. E. I., and Buono, M. R. (2022). Encrusted-barnacles on fossil cetacean bones as first evidence of reef stage of a whale-fall from shallow marine deposits, early Miocene of Patagonia, Argentina. *J. Taphon.* 16, 45–46.
- Farroni, N. D., Cuitiño, J. E. I., Lazo, D. G., and Buono, M. R. (2024). Taphonomic analysis of an articulated baleen whale (cetacea; mysticeti) from upper Miocene inner shelf deposits of península valdés, patagonia, Argentina. *Palaio* 39, 97–112. doi:10.2110/palo.2022.039
- Freschi, A., and Raineri, G. (2014). I cetacei fossili mio-pliocenici conservati nel Museo Paleontologico "Il Mare Antico" di Salsomaggiore Terme (Parma). *Museol. Sci. Mem.* 13, 46–53.
- Gale, A. (2019). Correlation, age and significance of Turonian Chalk hardgrounds in southern England and northern France: the roles of tectonics, eustasy, erosion and condensation. *Cretac. Res.* 103, 104164. doi:10.1016/j.cretres.2019.06.010
- Glover, A., Higgs, N., Bagley, P., Carlsson, R., Davies, A., Kemp, K., et al. (2010). A live video observatory reveals temporal processes at a shelf-depth whale-fall. *Cah. Biol. Mar.* 51, 375–381.
- Glover, A. G., Wiklund, H., Taboada, S., Avila, C., Cristobo, J., Smith, C. R., et al. (2013). Bone-eating worms from the Antarctic: the contrasting fate of whale and wood remains on the Southern Ocean seafloor. *Proc. R. Soc. B* 280, 20131390. doi:10.1098/rspb.2013.1390
- Goedert, J. L., Squires, R. L., and Barnes, L. G. (1995). Paleoecology of whale-fall habitats from deep-water Oligocene rocks, Olympic Peninsula, Washington state. *Palaeogeogr. Palaeoclim.* 118, 151–158. doi:10.1016/0031-0182(94)00139-y
- Gowender, R., Bisconti, M., and Chinsamy, A. (2016). Late miocene-early Pliocene baleen whale assemblage from langebaanweg, west coast of South Africa (mammalia, cetacea, mysticeti). *Alcheringa* 40, 542–555. doi:10.1080/03115518.2016.1159413
- Heijne, J., Klein, N., and Sander, P. M. (2019). The uniquely diverse taphonomy of the marine reptile skeletons (Sauropterygia) from the Lower Muschelkalk (Anisian) of Winterswijk, The Netherlands. *PalZ* 93, 69–92. doi:10.1007/s12542-018-0438-0
- Higgs, N. D., Glover, A. G., Dahlgren, T. G., Smith, C. R., Fujiwara, Y., Pradillon, F., et al. (2014). The morphological diversity of *Osedax* worm borings (Annelida: siboglinidae). *J. Mar. Biol. Assoc. U. K.* 94, 1429–1439. doi:10.1017/s0025315414000770
- Higgs, N. D., Little, C. T. S., Glover, A. G., Dahlgren, T. G., Smith, C. R., and Dominici, S. (2012). Evidence of *Osedax* worm borings in Pliocene (~3 Ma) whale bone from the mediterranean. *Hist. Biol.* 24, 269–277. doi:10.1080/08912963.2011.621167
- Jamison-Todd, S., Upchurch, P., and Mannion, P. D. (2023). The prevalence of invertebrate bioerosion on Mesozoic marine reptile bone from the Jurassic and Cretaceous of the United Kingdom: new data and implications for taphonomy and environment. *Geol. Mag.* 160, 1701–1710. doi:10.1017/s0016756823000651
- Jenkins, R. G., Kaim, A., Amano, K., Sakurai, K., and Matsubara, K. (2018). A new Miocene whale-fall community dominated by the bathymodiolin mussel *Adipicola* from the Hobetsu area, Hokkaido, Japan. *Paleont. Res.* 22, 105–111. doi:10.2517/2017p0006
- Kaim, A., Kobayashi, Y., Echizenya, H., Jenkins, R. G., and Tanabe, K. (2008). Chemosynthesis-based associations on cretaceous plesiosaurid carcasses. *Acta palaeont. Pol.* 53, 97–104. doi:10.4202/app.2008.0106
- Kiel, S., Amano, K., Hikida, Y., and Jenkins, R. G. (2009). Wood-fall associations from late cretaceous deep-water sediments of hokkaido, Japan. *Lethaia* 42, 74–82. doi:10.1111/j.1502-3931.2008.00105.x
- Kiel, S., and Goedert, J. L. (2006). Deep-sea food bonanzas: early Cenozoic whale-fall communities resemble wood-fall rather than seep communities. *Proc. R. Soc. B Biol. Sci.* 273, 2625–2632. doi:10.1098/rspb.2006.3620

- Kiel, S., Goedert, J. L., Kahl, W.-A., and Rouse, G. W. (2010a). Fossil traces of the bone-eating worm *Osedax* in early Oligocene whale bones. *PNAS* 107, 8656–8659. doi:10.1073/pnas.1002014107
- Kiel, S., Kahl, W.-A., and Goedert, J. L. (2010b). *Osedax* borings in fossil marine bird bones. *Naturwissenschaften* 98, 51–55. doi:10.1007/s00114-010-0740-5
- Li, Q., Liu, Y., Li, G., Wang, Z., Zheng, Z., Sun, Y., et al. (2022). Review of the impact of whale fall on biodiversity in deep-sea ecosystems. *Front. Ecol. Evol.* 10, 885572. doi:10.3389/fevo.2022.885572
- Lin, C. H., Brzobohaty, R., Nolf, D., and Girone, A. (2017). Tortonian teleost otoliths from northern Italy: taxonomic synthesis and stratigraphic significance. *Euro. J. Taxon.* 322, 1–44. doi:10.5852/ejt.2017.322
- Lundsten, L., Paull, C. K., Schlining, K. L., McGann, M., and Ussler, W. (2010a). Biological characterization of a whale-fall near Vancouver Island, British Columbia, Canada. *Deep-Sea Res. I* 57, 918–922. doi:10.1016/j.dsr.2010.04.006
- Lundsten, L., Schlining, K. L., Frasier, K., Johnson, S. B., Kuhnz, L. A., Harvey, J. B. J., et al. (2010b). Time-series analysis of six whale-fall communities in Monterey Canyon, California, USA. *Deep. Res. I* 57, 1573–1584. doi:10.1016/j.dsr.2010.09.003
- Marasti, R. (1973). La fauna tortoniana del Torrente Stirone (Limite Parmense - Piacentino). *Boll. Soc. Pal. It.* 12, 76–120.
- Monegatti, P., and Raffi, S. (2010). The Messinian marine molluscs record and the dawn of the eastern Atlantic biogeography. *Palaeogeogr. Palaeoclim. Palaeoecol.* 297, 1–11. doi:10.1016/j.palaeo.2010.06.023
- Pirrone, C. A., Buatois, L. A., and Bromley, R. G. (2014). Ichnotaxobases for bioerosion trace fossils in bones. *J. Paleont.* 88, 195–203. doi:10.1666/11-058
- Pyenson, N. D., and Haasl, D. M. (2007). Miocene whale-fall from California demonstrates that cetacean size did not determine the evolution of modern whale-fall communities. *Biol. Lett.* 3, 709–711. doi:10.1098/rsbl.2007.0342
- Ruggiero, E. T., and Bittner, M. A. (2008). Bioerosion on brachiopod shells – a Cenozoic perspective. *Earth Environ. Sci. Trans. Roy. Soc. Edinb.* 98, 369–378. doi:10.1017/S1755691007080371
- Scotton, R., Bigazzi, R., Casati, S., D'Amore, G., Di Marco, S., Foresi, L. M., et al. (2018). The “brunella” project: preparation and study of a mysticete from the early Pliocene of Tuscany. *Fossilia* 2018, 61–63. doi:10.32774/fosreppal.20.1810.156163
- Scotton, R., Bigazzi, R., D'Amore, G., Di Marco, S., Koenig, E., Nannini, P., et al. (2020). Il Progetto “Brunella”: principali attività preparatorie e strategie di comunicazione intorno ad un balenoteride pliocenico in Toscana. *Parva Nat.* 15, 85–133.
- Seki, A., and Jenkins, R. G. (2021). Pleistocene shallow-water whale-fall community from the omma Formation in Central Japan. *Paleont. Res.* 25, 191–200. doi:10.2517/2020pr024
- Smith, C. R., and Baco, A. R. (2003). Ecology of whale-falls at the deep-sea floor. *Oceanogr. Mar. Biol. Annu. Rev.* 41, 311–354.
- Smith, C. R., Glover, A. G., Treude, T., Higgs, N. D., and Amon, D. J. (2015). Whale-fall ecosystems: recent insights into ecology, paleoecology, and evolution. *Annu. Rev. Mar. Sci.* 7, 571–596. doi:10.1146/annurev-marine-010213-135144
- Treude, T., Smith, C. R., Wenzhöfer, F., Carney, E., Bernardino, A. F., Hannides, A. K., et al. (2009). Biogeochemistry of a deep-sea whale fall: sulfate reduction, sulfide efflux and methanogenesis. *Mar. Ecol. Progr. Ser.* 382, 1–21. doi:10.3354/meps07972
- Vai, G. B. (1988). “A field trip guide to the Romagna Apennine geology – the Lamone Valley,” in *Fossil vertebrates in the Lamone Valley, Romagna apennines. Field trip guidebook. International workshop, continental faunas at the mio-pliocene boundary, Faenza, March 28-31.* Editors C. De Giuli, and G. B. Vai, 7–37.
- Vinn, O., and Toom, U. (2016). A sparsely encrusted hardground with abundant Trypanites borings from the Llandoveri of the Velise River, western Estonia (Baltica). *Est. J. Earth Sci.* 65, 19–26. doi:10.3176/earth.2016.01
- Walne, P. R. (1958). Growth of oysters (*Ostrea edulis* L.). *J. Mar. Biol. Assoc. U. K.* 37, 591–602. doi:10.1017/s0025315400005634
- Zermani, A. (2001). *Biostratigrafia a Foraminiferi planctonici della successione Burdigaliano – Serravalliano del Torrente Stirone.* thesis (Parma: Università degli Studi di Parma).